G. M. Clark (1972). *The Structures of Non-Molecular Solids. A Coordinated Polyhedron Approach*, Applied Science Publishers.
R. C. Evans (1964). *An Introduction to Crystal Chemistry*, 2nd ed., Cambridge University Press.
S. M. Ho and B. E. Douglas (1969). *J. Chem. Ed.*, **46**, 207.
H. Krebs (1968). *Inorganic Crystal Chemistry*, McGraw-Hill.
I. Naray-Szabo (1969). *Inorganic Crystal Chemistry*, Akademiai Szabo.
E. Parthé (1964). *Crystal Chemistry of Tetrahedral Structures*, Gordon and Breach.
Structure Reports, International Union of Crystallography.
Ajit R. Verma and P. Krishna (1966). *Polymorphism and Polytypism in Crystals*, Wiley, New York.
R. Ward (1959). Mixed metal oxides, *Prog. Inorg. Chem.*, **1**, 465.
A. F. Wells (1984). 5th Ed. *Structural Inorganic Chemistry*, Oxford.
A. R. West (1975). *Z. Krist*, **141**, 422–436.
A. R. West and P. G. Bruce (1982). *Acta Cryst.*, **B38**, 1891–1896.
R. W. G. Wyckoff (1971). *Crystal Structures*, Vols 1 to 6, Wiley.

Chapter 8

Some Factors which Influence Crystal Structures

The previous chapter has dealt with the description and classification of crystal structures without paying too much attention to the reasons why a particular compound prefers one structure type to another. Crystal structures are influenced by a considerable number of factors—atom size, bonding type, electron configuration, etc.—and while each factor is understood fairly well in isolation, it is more difficult to assess the effect of all the factors in combination. Thus, it is a difficult, if not impossible, task to predict the structure of a new or unknown compound unless it falls into an obvious category such as a new spinel or perovskite phase. In this chapter, some of the factors that influence crystal structures are considered and an attempt made to review current ideas in crystal chemistry.

8.1 Preliminary survey

The structure adopted by a particular crystalline compound depends, to a first approximation, on three main factors: the general formula of the compound and the valencies of the elements present, the nature of the bonding between the atoms and the relative size of the atoms or ions.

8.1.1 General formulae, valencies and coordination numbers

Use of the term 'general formula' here refers to the relative number of atoms of each type that are present, without specifying what the atoms are, i.e. for a compound A_xB_y, the general formula gives the values of x and y without identifying A and B. For such a compound A_xB_y, the coordination numbers of A and B are related directly to the general formula. A general rule is that: *the coordination numbers of A and B are in the ratio y:x, provided that direct A–A or B–B contacts do not occur.* This applies to most ionic, polar and covalent polymeric materials but not to catenated compounds, such as polymers which have C—C bonds. Thus, for a compound AB_2, the coordination numbers of A(by B) and B(by A) are in the ratio of 2:1, as in SiO_2(4:2), TiO_2(6:3) and CaF_2 (8:4). Proof of this rule is not given here but after a little thought it should be obvious that it applies, at least to simple formulae, AB, AB_2, etc. The rule does not predict absolute coordination numbers for a given formula but it does place restrictions on the combination of coordination numbers that are possible in a structure.

The rule may be extended to more complex structures. In a compound $A_xB_yC_z$, in which A and B are cations coordinated only to anions, C, the *average* cation coordination number (CN) is related to the anion coordination number by

$$\frac{\text{Average cation CN}}{\text{Anion CN}} = \frac{z}{x+y} \tag{8.1}$$

in which the average cation CN is given by

$$\frac{x(\text{CN of A}) + y(\text{CN of B})}{x+y} \tag{8.2}$$

Substitution of (8.2) into (8.1) gives

$$x(\text{CN of A}) + y(\text{CN of B}) = z(\text{CN of C}) \tag{8.3}$$

The application of (8.3) can be seen in the following examples:

(a) Perovskite, $CaTiO_3$, contains octahedral Ti^{4+} and twelve coordinate Ca^{2+} ions. From (8.3), therefore, the anion CN is calculated to be six. The actual structure of perovskite is in agreement with this since oxygen is coordinated octahedrally to two Ti^{4+} and four Ca^{2+} ions.

(b) Spinel, $MgAl_2O_4$, contains tetrahedral Mg^{2+} and octahedral Al^{3+} ions. From (8.3), the oxygen CN is calculated to be four. This is correct since, in spinel, oxygen is tetrahedrally coordinated to three Al^{3+} and one Mg^{2+} ions.

This relationship between general formulae and coordination number is of little predictive value alone since it cannot be used in the absence of structural information. However, it does allow a certain degree of rationalization of formulae and coordination numbers and is useful for checking the anion CN in complex structures. It breaks down when bonding occurs between atoms of the same type, e.g. in $CdCl_2$ in which chlorine–chlorine contacts occur.

The above comments apply to the *relative* coordination numbers in a compound and take no account of the valency of the atoms. In molecular materials, the *absolute* coordination numbers are obviously controlled by valency since electron pair covalent bonds hold the molecules together. Unless multiple or partial bonds occur, the number of bonds to a particular atom in a molecule is equal to the coordination number and hence to the valency of that atom.

In non-molecular materials, however, the valency of an atom or ion does not have a direct bearing on coordination numbers and structure, apart from its obvious importance in controlling the general formula of the compound. Thus, the compounds in the series, LiF, MgO, ScN, TiC, all have the same general formula, AB, and the same crystal structure, that of rock salt. Coordination numbers are 6:6, therefore, but the valencies of the atoms increase from one in LiF to four in TiC. The type of bonding present certainly varies across the series, from ionic in LiF to essentially covalent in TiC, but the structure, given by the relative arrangement of atoms, is independent of atom valence.

8.1.2 Bonding

The nature of the bonding between atoms affects considerably the coordination numbers of the atoms and hence has a major influence on the crystal structure that is adopted. Broadly speaking, ionic bonding leads to structures with high symmetry and in which the coordination numbers are as high as possible. In this way, the net electrostatic attractive force which holds crystals together (and hence the lattice energy) is maximized. Covalent bonding, on the other hand, gives highly directional bonds in which one or all of the atoms present

has a definite preference for a certain coordination environment, irrespective of the other atoms that are present. The coordination numbers in covalently bonded structures are usually small and may be less than those in corresponding ionic structures which contain atoms of similar size to those in the covalent structure.

The type of bonding that occurs in a compound correlates fairly well with the position of the component atoms in the periodic table and, especially, with their electronegativity. Alkali and alkaline earth elements usually form essentially ionic structures (beryllium is sometimes an exception), especially in combination with smaller, more electronegative anions such as O^{2-} and F^-. Covalent structures occur especially with (a) small atoms of high valency which, in the cationic state, would be highly polarizing, e.g. B^{3+}, Si^{4+}, P^{5+}, S^{6+}, etc., and to a lesser extent with (b) large atoms which in the anionic state are highly polarizable, e.g. I^-, S^{2-}.

Most non-molecular compounds have bonding which is a mixture of ionic and covalent and, as discussed later, it is becoming possible to make quantitative assessments of the *ionicity* of a particular bond, i.e. the percentage of ionic character in the bond. An additional factor in some transition metal compounds is the occurrence of metallic bonding.

Some clear-cut examples of the influence of bonding type on crystal structure are as follows:

(a) *SrO, BaO, HgO.* SrO and BaO both have the rock salt structure with octahedrally coordinated M^{2+} ions. Based on size considerations alone, and if it were ionic, HgO would also be expected to have the same structure. However, mercury is only two coordinate in HgO and the structure may be regarded as covalent. Linear O—Hg—O segments occur in the structure and may be rationalized on the basis of *sp* hybridization of mercury. The ground state of atomic mercury is

$$(\text{Xe core})\ 4f^{14}\quad 5d^{10}\quad 6s^2$$

The first excited state, corresponding to mercury (II), is

$$(\text{Xe core})\quad 4f^{14}\quad 5d^{10}\quad 6s^1\quad 6p^1$$

Hybridization of the 6*s* and one 6*p* orbital gives rise to two, linear *sp* hybrid orbitals, each of which forms a normal, electron pair, covalent bond by overlap with an orbital on oxygen. Hence mercury has a CN of two in HgO.

(b) *AlF_3, $AlCl_3$, $AlBr_3$ and AlI_3.* These compounds show a smooth transition from ionic to covalent bonding as the electronegativity difference between the two elements decreases. Thus, AlF_3 is a high melting, essentially ionic solid with a distorted octahedral coordination of the Al^{3+} ions; its structure is related to that of ReO_3. $AlCl_3$ has a layered, polymeric structure in the solid state similar to the structure of $CrCl_3$, which is related to the $CdCl_2$ and CdI_2 structures. The bonds may be regarded as part ionic/part covelent. $AlBr_3$ and AlI_3 have molecular structures with dimeric units of formula Al_2X_6. Their structure and shape is shown in Fig. 7.10 and the bonding between aluminium and bromine or iodine is essentially covalent.

Halides of other elements, e.g. Be, Mg, Ga, In, also show variations in bond type and structure, depending on the halide. The trends are always the same; with the fluorides there is the largest difference in electronegativity between the two elements and these structures are the most ionic. With the other halides increasing covalent character occurs in the series, chloride–bromide–iodide.

8.1.3 Size

The relative size of the atoms in a compound has a major influence on the structure adopted, especially for more ionic structures. A guiding principle in ionic structures is that the coordination number of a particular ion is as large as possible, provided that it can be in contact with all of its neighbouring ions of opposite charge. The limiting situation occurs when a cation is too small to fit snugly into a particular hole in the anion array and a hypothetical structure in which a cation can rattle inside its hole is regarded as unstable. The limiting size of the interstitial hole in various anion arrays, e.g. f.c.c. and b.c.c., can be estimated, in theory, using the radius ratio rules (Section 8.2.3), but it must be stated that in practice there are many exceptions to the rules. The general relation between size and coordination number is clear, however; as the value of the ratio (cation radius/anion radius) increases, so the coordination number of the cation increases. A good example of this, and to which the radius ratio rules may apparently be applied successfully, is oxides, MO_2. With increasing size of M, the structure and coordination number changes in the sequence:

CO_2 (CN of C = 2)
SiO_2 (CN of Si = 4)
TiO_2 (CN of Ti = 6)
PbO_2 (CN of Pb = 8)

Other examples of this trend are:

BeF_2(SiO_2 str., CN = 4); MgF_2(TiO_2 str., CN = 6); CaF_2(CN = 8)
Rb_2O(CN = 4); Cs_2O(CN = 6)
BeO(ZnS str., CN = 4); MgO(NaCl str., CN = 6)

In molecular materials, however, size considerations are less important. This is partly because the coordination numbers in molecular materials are controlled by valency and partly because the covalent radii of elements do not show the same spread of values as do the ionic radii. Usually, the radii of a particular element are in the following sequence:

$$\text{Cation radius} < \text{covalent radius} < \text{anion radius}$$

although few elements can exist in all three states. Thus magnesium may be cationic or covalent in its compounds but never anionic, whereas fluorine may be covalent or anionic but never cationic. Examples of elements which may exist in all three states are hydrogen and iodine.

Because elements do not differ too much in their covalent radii (see Table 8.10 later), it is usually possible to satisfy the valence and bonding requirements of atoms in molecules without interference from size problems. For example, consider CI_4 which is a covalently bonded, tetrahedral molecule. The covalent radius of carbon is large enough that four covalent C—I bonds can form. If the structure were ionic, however, the C^{4+} ion (which does not exist, chemically) would be too small to be tetrahedrally coordinated by the large I^- ions.

8.2 Ionic structures

Purely ionic bonding in crystalline compounds is an idealized or extreme form of bonding which is rarely attained in practice. Even in structures that are regarded as essentially ionic, e.g. NaCl and CaO, there is usually a certain amount of covalent bonding between cation and anion which acts to reduce the charge on each. The degree of covalent bonding increases with increasing valence of the ions to the extent that ions with a *net* charge greater than + 1 or − 1 appear unlikely to exist. Thus, while NaCl may reasonably be represented as Na^+Cl^-, TiC (which also has the NaCl structure) certainly does not contain Ti^{4+} and C^{4-} ions and the main bonding type in TiC must be non-ionic. This brings us to a dilemma. Do we continue to use the ionic model in the knowledge that for many structures, e.g. Al_2O_3, $CdCl_2$, a large degree of covalent bonding must be present? If not, we must find an alternative model for the bonding. In this chapter, ionic bonding is given considerable prominence because of its apparent wide applicability and its usefulness as a *starting point* for describing structures which in reality have a considerable amount of covalent bonding. In Section 8.3 and 8.4, two methods of assessing the degree of covalent character in 'ionic structures' are discussed.

8.2.1 Ions and ionic radii

It is difficult to imagine discussing crystal chemistry without having information available on the sizes of ions in crystals. However, crystal chemistry is currently undergoing a minor revolution in that the long-established tables of ionic radii of Pauling (1928), Goldschmidt and others are now thought to be seriously in error; at the same time, our concepts of ions and ionic structures are also undergoing revision. In recent compilations of ionic radii, e.g. of Shannon and Prewitt (1969, 1970), cations are shown as being larger and anions smaller than previously thought. For example, Pauling radii of Na^+ and F^- are 0.98 and 1.36 Å, respectively, whereas Shannon and Prewitt give values of 1.14 to 1.30 Å, depending on the coordination number, for Na^+ and 1.19 Å for F^-.

These changes have arisen largely because, with modern, high quality X-ray diffraction work it is possible to obtain fairly accurate maps of the distribution of electron density throughout ionic crystals. Thus, one can effectively 'see' ions and tell something about their size, shape and nature. In Fig. 8.1 is shown an electron density 'contour map' (see Chapter 5, Section 5.5.6) for LiF for a section passing through the structure parallel to one unit cell face. The map therefore passes

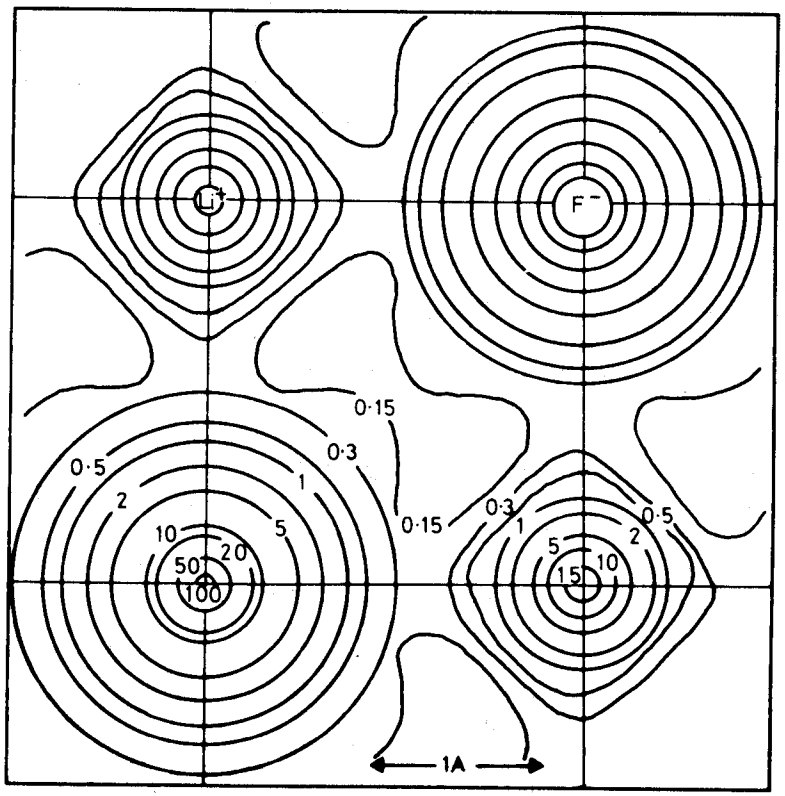

Fig. 8.1 Electron density contour map of LiF: a section through part of the unit cell face. The electron density (electrons $Å^{-3}$) is constant along each of the contour lines. (From Krug, Witte and Welfel, 1955)

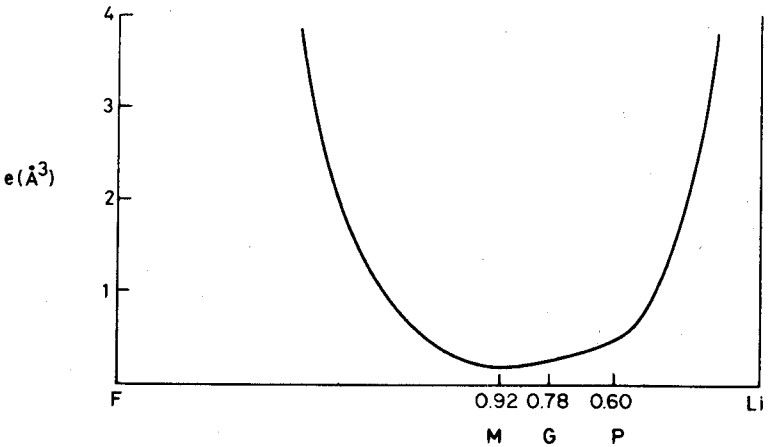

Fig. 8.2 Variation of electron density along the line connecting adjacent Li and F nuclei in LiF. (From Krebs, 1968). P = Pauling radius of Li^+, G = Goldschmidt radius, M = minimum in electron density

through the centres of Li^+ and F^- ions located on the (100) planes. In Fig. 8.2 is shown the variation of electron density with distance along the line that connects adjacent Li^+ and F^- ions. From Figs 8.1 and 8.2 and similar diagrams for other structures (Fig. 5.39 a, for NaCl), the following conclusions about ions in crystals may be drawn:

(a) Ions are essentially spherical.
(b) Ions may be regarded as composed of two parts: a central core in which most of the electron density is concentrated and an outer sphere of influence which contains very little electron density.
(c) Assignment of radii to ions is difficult; even for ions which are supposedly in contact, it is not obvious (Fig. 8.2) where one ion ends and another begins.

Conclusion (b) is in contrast to the oft-stated assumption that 'ions can be treated as charged, incompressible, non-polarizable spheres'. Certainly, ions are charged, but they cannot be regarded as spheres with a clearly defined radius. Their electron density does not decrease abruptly to zero at a certain distance from the nucleus but decreases only gradually with increasing radius. Instead of being incompressible, ions are probably quite elastic, by virtue of flexibility in the outer sphere of influence of an ion while the inner core remains unchanged. This is necessary in order to explain variations of apparent ionic radii with coordination number and environment (see later). Within limits, ions can therefore expand or contract as the situation demands.

From Figs 8.1 and 8.2, most of the electron density is concentrated close to the nuclei of the ions; in a crystal, therefore, most of the total volume is essentially free space and contains relatively little electron density.

The difficulties involved in determining ionic radii arise because, between adjacent anions and cations, the electron density passes through a broad minimum. For LiF (Fig. 8.2), the radii for Li^+ given by Pauling and Goldschmidt are marked together with the value which corresponds to the minimum in the electron density along the line connecting Li^+ and F^-. Although the values of these radii vary from 0.60 to 0.92 Å, all lie within the broad electron density minimum of Fig. 8.2.

The many methods that have been used in the past to estimate ionic radii will not be discussed here. In spite of the difficulties involved in determining absolute radii, it is necessary to have a set of radii for reference. Fortunately, most sets of radii are *additive* and *self-consistent*; provided one does not mix radii from different tabulations it is possible to use any set of radii to evaluate interionic distances in crystals with reasonable confidence. Shannon and Prewitt give two sets of radii: one is based on $r_0 = 1.40$ Å and is similar to Pauling, Goldschmidt, etc.; the other is based on $r_{F^-} = 1.19$ Å (and $r_{O^{2-}} = 1.26$ Å) and is related to the values determined from X-ray electron density maps. Both sets are comprehensive for cations in their different coordination environments but only pertain to oxides and fluorides. We choose here to use the Shannon and Prewitt set based on $r_{F^-} = 1.19$ Å and $r_{O^{2-}} = 1.26$ Å. Cation radii are shown in graphical form in

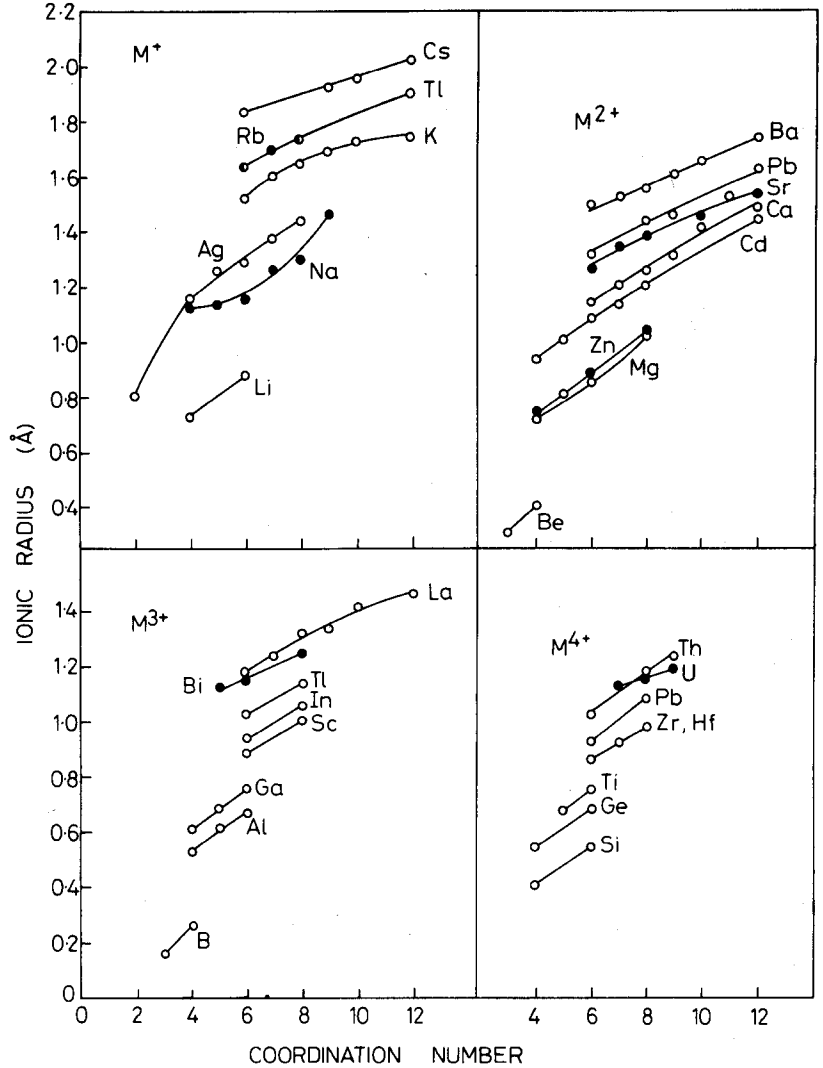

Fig. 8.3 Ionic radii as a function of coordination number for cations M^+ to M^{4+}. (From Shannon and Prewitt, 1969, 1970.) Data based on $r_{F^-} = 1.19$ Å (and $r_{O^{2-}} = 1.26$ Å)

Fig. 8.3 as a function of cation coordination number. Radii are given for ions M^+ to M^{4+}; it should be stressed that the more highly charged ions are unlikely to exist as such in the purely ionic state but probably have their positive charged reduced by polarization of the anion and consequent partial covalent bonding between cation and anion.

The following trends in ionic radii, with position in the periodic table, formal charge and coordination number, occur:

(a) For the *s*- and *p*-block elements, radii increase with atomic number for any vertical group, e.g. octahedrally coordinated alkali ions.
(b) For any isoelectronic series of cations, the radius decreases with increasing charge, e.g. Na^+, Mg^{2+}, Al^{3+} and Si^{4+}.
(c) For any element which can have variable oxidation states, the cation radius decreases with increasing oxidation state, e.g. V^{2+}, V^{3+}, V^{4+}, V^{5+}.
(d) For an element which can have various coordination numbers, the cationic radius increases with increasing coordination number.
(e) The 'lanthanide contraction' occurs as follows: across the lanthanide series, ions with the same charge but increasing atomic number show a reduction in size due to the ineffective shielding of the nuclear charge by the *d* and, especially, *f* electrons, e.g. octahedral radii, La^{3+} (1.20 Å) ... Eu^{3+} (1.09 Å) ... Lu^{3+} (0.99 Å). Similar effects occur across some series of transition metal ions.
(f) The radius of a particular transition metal ion is smaller than that of the corresponding main group ion for the reasons given in (e), e.g. Rb^+ (1.63 Å) and Ag^+ (1.29 Å) or Ca^{2+} (1.14 Å) and Zn^{2+} (0.89 Å).
(g) Certain pairs of elements positioned diagonally to one another in the periodic table have similar ionic size (and chemistry), e.g. Li^+ (0.88 Å) and Mg^{2+} (0.86 Å). This is due to a combination of effects (a) and (b).

8.2.2 Ionic structures—general principles

Consider the following as a guide to ionic structures:

(a) Ions are regarded as charged, elastic .and polarizable spheres.
(b) Ionic structures are held together by electrostatic forces and, therefore, are arranged so that cations are surrounded by anions, and vice versa.
(c) In order to maximize the net electrostatic attraction between ions in a structure (i.e. the lattice energy), coordination numbers are as high as possible, provided that the central ion maintains contact (via its sphere of influence) with all its neighbouring ions of opposite charge.
(d) Next nearest neighbour interactions are of the anion–anion and cation–cation type and are repulsive. Like ions arrange themselves to be as far apart as possible, therefore, and this leads to structures of high symmetry with a maximized volume.
(e) Local electroneutrality prevails, i.e. the valence of an ion is equal to the sum of the electrostatic bond strengths between it and adjacent ions of opposite charge.

Point (a) has been considered in the previous section; ions are obviously charged, are elastic because their size varies with coordination number and are polarizable when departures from purely ionic bonding occurs. For example, the electron density map for LiF (Fig. 8.1) shows a small distortion from spherical shape in the outer part of the sphere of influence of the Li^+ ion, and this may be

attributed to the occurrence of a small amount of covalent bonding between Li^+ and F^-.

Points (b) and (d) infer that the forces which hold ionic crystals together and the net energy of the interaction between the ions are the same as would be obtained by regarding the crystal as a three-dimensional array of point charges and considering the net coulombic energy of the array. From Coulomb's Law, the force F between two ions of charge Z_+e and Z_-e, separated by distance r, is given by

$$F = \frac{(Z_+e)(Z_-e)}{r^2} \tag{8.4}$$

A similar equation applies to each pair of ions in the crystal and evaluation of the resulting force between all the ions leads to the lattice energy of the crystal (Section 8.2.5).

Point (c) includes the proviso that nearest neighbour ions should be 'in contact'. Given the nature of electron density distributions in ionic crystals (Figs 8.1 and 8.2), it is hard to quantify what is meant by 'in contact'. It is nevertheless an important factor since, although the apparent size of ions varies with coordination number, most ions, smaller ones especially, appear to have a maximum coordination number; for Be^{2+} this is four and for Li^+ it is six. Ions are flexible, therefore, but expand or contract only within fairly narrow limits.

The idea of *maximizing* the volume of ionic crystals, point (d) is rather unexpected (Brunner; O'Keeffe) since one is accustomed to regarding ionic structures and derivative close packed structures, expecially, as having *minimum* volume. There is no conflict, however. The prime bonding force in ionic crystals is the nearest neighbour cation–anion *attractive* force and this force is maximized at a small cation–anion separation (when ions become too close, additional repulsive forces come into play, Section 8.2.5, thereby reducing the net attractive force). Superposed on this is the effect of next nearest neighbour *repulsive* forces between like ions. With the constraints that (a) cation–anion distances be as short as possible and (b) coordination numbers be as large as possible, like ions arrange themselves to be as far apart as possible in order to reduce their mutual repulsion. This leads to regular and highly symmetrical arrays of like ions. It has been shown (O'Keeffe) that such regular arrays of like ions tend to have maximized volumes and that, by distorting the structures, a reduction in volume is possible, at least in principle.

An excellent example of a structure whose volume is maximized is rutile (see Chapters 6 and 7). The buckling of the oxide layers (Fig. 6.16) causes the coordination number of oxygen to be reduced from 12 (as in h.c.p.) to 11 (as in p.t.p.). The coordination of titanium by oxygen, and vice versa, is unaffected by this distortion but the overall volume of the structure increases by 2 to 3 per cent.

Point (e) is Pauling's electrostatic valence rule, the second of a set of rules formulated by Pauling for ionic crystals. Basically, the rule means that the charge on a particular ion, e.g. an anion, must be balanced by an equal and opposite charge on the surrounding cations. However, since these cations are also shared

with other anions, it is necessary to estimate the amount of positive charge that is effectively associated with each cation–anion bond. For a cation M^{m+} surrounded by n anions, X^{x-}, the *electrostatic bond strength* (e.b.s.) of the cation–anion bonds is defined as

$$\text{e.b.s.} = \frac{m}{n} \tag{8.5}$$

For each anion, the sum of the electrostatic bond strengths of the surrounding cations must balance the negative charge on the anion, i.e.

$$\sum \frac{m}{n} = x \tag{8.6}$$

For example:

(a) Spinel, $MgAl_2O_4$, contains octahedral Al^{3+} and tetrahedral Mg^{2+} ions; each oxygen is surrounded tetrahedrally by three Al^{3+} ions and one Mg^{2+} ion. We can check that this must be so, as follows:

For Mg^{2+}: e.b.s. $= \frac{2}{4} = \frac{1}{2}$

For Al^{3+}: e.b.s. $= \frac{3}{6} = \frac{1}{2}$

Therefore,

$$\sum \text{e.b.s.}(3Al^{3+} + 1Mg^{2+}) = 2$$

(b) We can show that three SiO_4 tetrahedra cannot share a common corner in silicate structures:

For Si^{4+}: e.b.s. $= \frac{4}{4} = 1$

Therefore, for an oxygen that bridges two SiO_4 tetrahedra, $\sum$e.b.s. $= 2$, which is acceptable. However, three tetrahedra sharing a common oxygen would give $\sum$e.b.s. $= 3$ for that oxygen, which is quite unacceptable.

This rule of Pauling's provides an important guide to the kinds of polyhedral linkages that are and are not possible in crystal structures. In Table 8.1 is given a list of some common cations with their formal charge, coordination number and electrostatic bond strength. In Table 8.2 are listed some allowed and unallowed combinations of polyhedra about a common oxide ion, together with some examples of the allowed combinations. Many other combinations are possible and the reader may like to deduce some, bearing in mind that there are also topological restrictions on the number of possible polyhedral combinations; thus the maximum number of octahedra that can share a common corner is six (as in rock salt), etc.

Pauling's third rule is concerned with the topology of polyhedra and has been considered in the previous chapter. Pauling's first rule states: 'A coordinated polyhedron of anions is formed about each cation, the cation–anion distance

Table 8.1 *Electrostatic bond strengths of some cations*

Cation with formal charge	Coordination number	Electrostatic bond strength
Li^+	4,6	$\frac{1}{4}, \frac{1}{6}$
Na^+	6,8	$\frac{1}{6}, \frac{1}{8}$
Be^{2+}	3,4	$\frac{2}{3}, \frac{1}{2}$
Mg^{2+}	4,6	$\frac{1}{2}, \frac{1}{3}$
Ca^{2+}	8	$\frac{1}{4}$
Zn^{2+}	4	$\frac{1}{2}$
Al^{3+}	4,6	$\frac{3}{4}, \frac{1}{2}$
Cr^{3+}	6	$\frac{1}{2}$
Si^{4+}	4	1
Ge^{4+}	4,6	$1, \frac{2}{3}$
Ti^{4+}	6	$\frac{2}{3}$
Th^{4+}	8	$\frac{1}{2}$

Table 8.2 *Allowed and unallowed combinations of corner-sharing oxide polyhedra*

Allowed	Example	Unallowed
$2SiO_4$ tet.	Silica	$> 2SiO_4$ tet.
$1MgO_4$tet. + $3AlO_6$oct.	Spinel	$3AlO_4$ tet.
$1SiO_4$tet. + $3MgO_6$oct.	Olivine	$1SiO_4$tet. + $2AlO_4$tet.
$8LiO_4$tet.	Li_2O	$4TiO_6$ oct.
$2TiO_6$oct. + $4CaO_{12}$dod.	Perovskite	
$3TiO_6$oct.	Rutile	

being determined by the radius sum and the coordination number of the cation by the radius ratio.' The idea that cation–anion distances are determined by the radius sum is implicit to every tabulation of ionic radii since a major objective of such tabulations is to be able to predict, correctly, interatomic distances. Let us now consider coordination numbers and *the radius ratio rules.*

8.2.3 The radius ratio rules

In ideally ionic crystal structures, the coordination numbers of the ions are determined largely by electrostatic considerations. Cations surround themselves with as many anions as possible, and vice versa. This maximizes the electrostatic attractions between neighbouring ions of opposite charge and hence maximizes the lattice energy of the crystal (see later). This requirement led to the formulation of the *radius ratio rules* for *ionic structures* in which the ions and the structure adopted for a particular compound depend on the *relative* sizes of the ions. There are two guidelines to be followed. First, a cation must be in contact with its

anionic neighbours and so this places a *lower* limit on the size of cation which may occupy a particular site. A situation in which a cation may 'rattle' inside its anion polyhedron is assumed to be unstable. Second, neighbouring anions may or may not be in contact. Using these guidelines, one may calculate the range of cation sizes that can occupy the various interstitial sites in an anion array, as follows.

For a face centred cubic array (e.g. NaCl structure), in which the anions are in contact, octahedral cation sites have a minimum radius r_m, given from Fig. 8.4 by

$$(2r_x)^2 + (2r_x)^2 = [2(r_m + r_x)]^2$$

and therefore,

$$\frac{r_m}{r_x} = \sqrt{2} - 1 = 0.414$$

Atoms 1, 2, 3 and 4, 5, 6 belong to adjacent close packed layers and an octahedral site lies midway between. Atoms 1, 2 and 3 are in contact, as also are 4, 5 and 6. Between the layers, atoms 2 and 3 are in contact with 4 and 5. For smaller cations (i.e. $r_m/r_x < 0.414$) the cation could not be in contact with all six anionic nearest neighbours and, therefore, according to the theory, a structure with lower cation coordination number would result. (Note that, in practice, structures *do* occur in

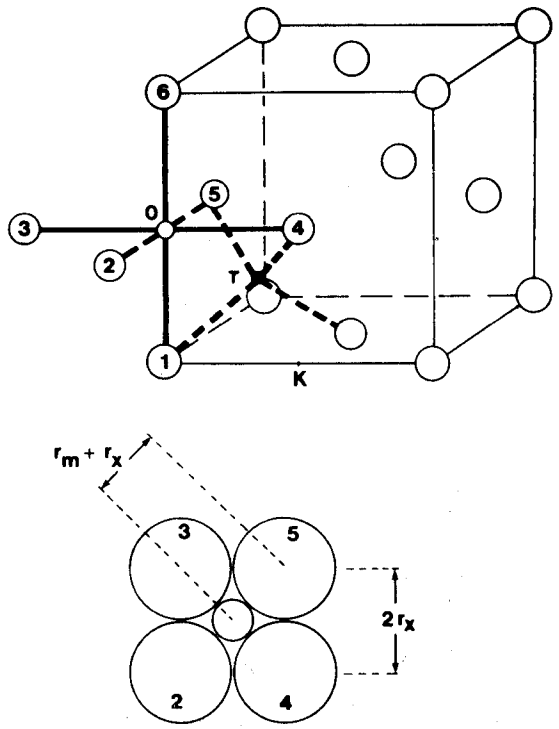

Fig. 8.4 Octahedral and tetrahedral cation sites in a face centred cubic (cubic close packed) anion array

which a cation is obviously too small for its particular site, e.g. the sodium ions in the solid electrolyte, β-alumina, occupy very large sites.)

For radius ratios > 0.414 the cation would push the anions apart and this happens increasingly up to a radius ratio of 0.732. At and above this value, the cation is sufficiently large to have eight anionic neighbours, all of which are in contact with the cation. The CsCl structure (Fig. 7.20) has eight-coordinate ions. Here,

$$[2(r_m + r_x)]^2 = (\text{cube body diagonal})^2$$
$$= 3(2r_x)^2$$

Therefore,

$$\frac{r_m}{r_x} = \sqrt{3} - 1 = 0.732$$

For tetrahedral coordination (Fig. 8.4), distance 5 – *K* is the body diagonal of a small cube and is equal to $2(r_m + r_x)$. Therefore,

$$(2r_x)^2 + (\sqrt{2}r_x)^2 = [2(r_m + r_x)]^2$$

and

$$\frac{r_m}{r_x} = \tfrac{1}{2}(\sqrt{6} - 2) = 0.225$$

The minimum radius ratios for various coordination numbers are given in Table 8.3. With the exception of CN = 8, all are applicable to close packed structures. Note that CN = 5 is absent from the table; in close packed structures, it is not possible to have a coordination number of five in which all M—X bonds are of the same length.

The radius ratio rules have had a limited amount of success in predicting trends in coordination number and structure type and at best can only be used as a general guideline. Radius ratios depend very much on which table of ionic radii is consulted and there appears to be no clear advantage in using either one of the more traditional sets or the modern set of values based on X-ray diffraction results. For example, for RbI, $r+/r- = 0.69$ or 0.80, according to the tables based on $r_{O^{2-}} = 1.40$ and 1.26 Å, respectively. Thus one value would predict six-coordination (rock salt), as observed, but the other predicts eight-coordination (CsCl). On the other hand, LiI has $r+/r- = 0.28$ and 0.46, according to the

Table 8.3 *Minimum radius ratios for different cation coordination numbers*

Coordination	Minimum $r_m:r_x$
Linear, 2	—
Trigonal, 3	0.155
Tetrahedral, 4	0.225
Octahedral, 6	0.414
Cubic, 8	0.732

Table 8.4 *Structures and radius ratios of oxides, MO_2*

Oxide	Calculated radius ratio*		Observed structure type	
CO_2	~0.1	(CN = 2)	Molecular	(CN = 2)
SiO_2	0.32	(CN = 4)	Silica	(CN = 4)
GeO_2	0.43	(CN = 4)	Silica	(CN = 4)
	0.54	(CN = 6)	Rutile	(CN = 6)
TiO_2	0.59	(CN = 6)	Rutile	(CN = 6)
SnO_2	0.66	(CN = 6)	Rutile	(CN = 6)
PbO_2	0.73	(CN = 6)	Rutile	(CN = 6)
HfO_2	0.68	(CN = 6)	Fluorite	(CN = 8)
	0.77	(CN = 8)		
CeO_2	0.75	(CN = 6)	Fluorite	(CN = 8)
	0.88	(CN = 8)		
ThO_2	0.95	(CN = 8)	Fluorite	(CN = 8)

* Since cation radii vary with coordination number, as shown in Fig. 8.3, radius ratios may be calculated for different coordination numbers. The coordination numbers used here are shown in parentheses. Calculations are based on $r_{O^{2-}} = 1.26$ Å.

tables based on $r_{O^{2-}} = 1.40$ and 1.26 Å, respectively. One value predicts tetrahedral coordination and the other octahedral (as observed). For the larger cations, especially caesium, $r+/r- > 1$, and it is perhaps more realistic to consider instead the inverse ratio, $r-/r+$, for CsF.

A more convincing example of the relevance of radius ratio rules is provided by oxides and fluorides of general formula, MX_2. Possible structure types, with their cation coordination numbers, are silica (4), rutile (6) and fluorite (8). A selection of oxides in each group is given in Table 8.4, together with the radius ratios calculated from Fig. 8.3 (based on $r_{O^{2-}} = 1.26$ Å). Changes in coordination number are expected to occur at radius ratios of 0.225, 0.414 and 0.732. Bearing in mind that the calculated radius ratio values depend on the particular table of radii that is consulted, the agreement between theory and practice is reasonable. For example, GeO_2 is polymorphic and can have both silica and rutile structures; the radius ratio calculated for tetrahedral coordination of germanium is borderline between the values predicted for CN = 4 and 6.

8.2.4 Borderline radius ratios and distorted structures

The structural transition from CN = 4 to 6 which occurs with increasing cation size is often clear-cut. A good example is provided by GeO_2 which has a borderline radius ratio and which also exhibits polymorphism. Both polymorphs have highly symmetric structures; one has a silica-like structure with CN = 4 and the other has a rutile structure with CN = 6. Polymorphs with CN = 5 do not occur with GeO_2.

In other cases of borderline radius ratios, however, distorted polyhedra and/or

coordination numbers of 5 are observed. Thus V^{5+} (radius ratio = 0.39 for CN = 4 or radius ratio = 0.54 for CN = 6) has an environment in one polymorph of V_2O_5 which is a gross distortion of octahedral; five V—O bonds are of reasonable length, in the range 1.5 to 2.0 Å, but the sixth bond is much longer, 2.8 Å, and the coordination is better regarded as distorted square pyramidal. It appears that V^{5+} is rather small to happily occupy an octahedral site and that, instead, a structure occurs which is transitional between tetrahedral and octahedral. Similar types of distortions occur between CN = 6 and 8. Thus, ZrO_2 has a borderline radius ratio (0.68 for CN = 6; 0.78 for CN = 8) and although it may have the fluorite structure at very high temperatures (> 2000 °C), with a CN of 8 for zirconium, in its normal form at room temperature as the mineral baddleyite, zirconium has a CN of 7.

Less severe distortions occur in cases where a cation is only slightly too small for its anion environment. The regular anion coordination is maintained but the cation may rattle or undergo small displacements within its polyhedron. In, for example, $PbTiO_3$ (radius ratio for Ti = 0.59 for CN = 6), titanium may undergo displacement by ~ 0.2 Å off the centre of its octahedral site towards one of the corner oxygens. The direction of displacement may be reversed under the action of an applied electric field and this gives rise to the important property of ferroelectricity (Chapter 15).

The concept of 'maximum contact distance' has been proposed by Dunitz and Orgel (1960). If the metal–anion distance increases above this distance then the cation is free to rattle. If the metal–anion distance decreases the metal ion is subjected to compression. However, the maximum contact distance does not correspond to the sum of ionic radii, as they are usually defined, and this is a difficult concept to quantify.

8.2.5 Lattice energy of ionic crystals

Ionic crystals may be regarded as regular three-dimensional arrangements of point charges. The forces that hold the crystals together are entirely electrostatic in origin and may be calculated by summing all the electrostatic repulsions and attractions in the crystal. The *lattice energy*, U, of a crystal is defined as the net potential energy of the arrangement of charges that forms the structure. It is equivalent to the energy required to sublime the crystal and convert it into a collection of gaseous ions, e.g.

$$NaCl(s) \rightarrow Na^+(g) + Cl^-(g), \qquad \Delta H = U$$

The value of U depends on the crystal structure that is adopted, the charge on the ions and the internuclear separation between the anion and cation.

Two principal kinds of force are involved in determining the crystal structure of ionic materials:

(a) The electrostatic forces of attraction and repulsion between ions. Two ions M^{z+} and X^{z-} separated by a distance, r, experience an attractive force, F,

given by Coulomb's Law:

$$F = \frac{Z_+ Z_- e^2}{r^2} \tag{8.4}$$

and their coulombic potential energy, V, is given by

$$V = \int_{\infty}^{r} F\,\mathrm{d}r = -\frac{Z_+ Z_- e^2}{r} \tag{8.7}$$

(b) Short range repulsive forces which are important when atoms or ions are so close together that their electron clouds begin to overlap. Born suggested that this repulsive energy has the form:

$$V = \frac{B}{r^n} \tag{8.8}$$

where B is a constant and the Born exponent, n, has a value in the range 5 to 12. Because n is large, V falls rapidly to zero with increasing r.

The lattice energy, U, of a crystal may be calculated by combining the net electrostatic attraction and the Born repulsion energies and finding the internuclear separation, r_e, which gives the maximum U value. The procedure is as follows:

Consider the NaCl structure (Fig. 7.13a). Between each pair of ions in a crystal there is an electrostatic interaction given by equation (8.4). We wish to sum all such interactions which occur in the crystal and calculate the net attractive energy. Let us first consider one particular ion, e.g. Na^+ in the body centre of the unit cell (Fig. 7.13a), and calculate the interaction between it and its neighbours. Its nearest neighbours are six Cl^- ions in the face centre positions and at a distance r ($2r$ is the value of the unit cell edge). The attractive potential energy (ignoring for the moment $Cl^- - Cl^-$ repulsions) is given by

$$V = -6\frac{e^2 Z_+ Z_-}{r} \tag{8.9}$$

The next nearest neighbours to the Na^+ ion are twelve Na^+ ions arranged at the edge centre positions of the unit cell, i.e. at a distance $\sqrt{2}r$; this gives a repulsive potential energy term

$$V = +12\frac{e^2 Z_+ Z_-}{\sqrt{2}r} \tag{8.10}$$

The third nearest neighbours are eight Cl^- ions at the cube corners and distance $\sqrt{3}r$; these are attracted to the central Na^+ ion according to

$$V = -8\frac{e^2 Z_+ Z_-}{\sqrt{3}r} \tag{8.11}$$

Table 8.5 *Madelung constants for some simple structures*

Structure type	A
Rock salt	1.748
CsCl	1.763
Wurtzite	1.641
Sphalerite	1.638
Fluorite	5.039
Rutile	4.816

The net attractive energy between our Na^+ ion and all other ions in the crystal is given by an infinite series:

$$V = -\frac{e^2 Z_+ Z_-}{r}\left(6 - \frac{12}{\sqrt{2}} + \frac{8}{\sqrt{3}} - \frac{6}{\sqrt{4}} + \cdots\right) \tag{8.12}$$

This summation is repeated for each ion in the crystal, i.e. for $2N$ ions per mole of NaCl. Since each ion pair interaction is thereby counted twice it is necessary to divide the final value by 2, giving

$$V = -\frac{e^2 Z_+ Z_-}{r} NA \tag{8.13}$$

where the *Madelung constant*, A, is the numerical value of the series summation in parentheses in equation (8.12). The Madelung constant depends only on the geometrical arrangement of point charges. It has the same value, 1.748, for all compounds with the rock salt structure. Values of A for some other simple structure types are given in Table 8.5.

If equation (8.13) represented the only factor involved in the lattice energy, the structure would collapse in on itself since $V \propto 1/r$ (Fig. 8.5). This catastrophe is avoided by the mutual repulsion between ions, of whatever charge, when they become too close, and is given by equation (8.8). The dependence of this repulsive force on r is also shown schematically in Fig. 8.5. The total energy of the crystal, the lattice energy U, is given by summing equations (8.8) and (8.13) and differentiating with respect to r to find the maximum U value and equilibrium interatomic distance, r_e; i.e.

$$U = -\frac{e^2 Z_+ Z_- NA}{r} + \frac{BN}{r^n} \tag{8.14}$$

Therefore,

$$\frac{\mathrm{d}U}{\mathrm{d}r} = \frac{e^2 Z_+ Z_- NA}{r^2} - \frac{nBN}{r^{n+1}} \tag{8.15}$$

When

$$\frac{\mathrm{d}U}{\mathrm{d}r} = 0$$

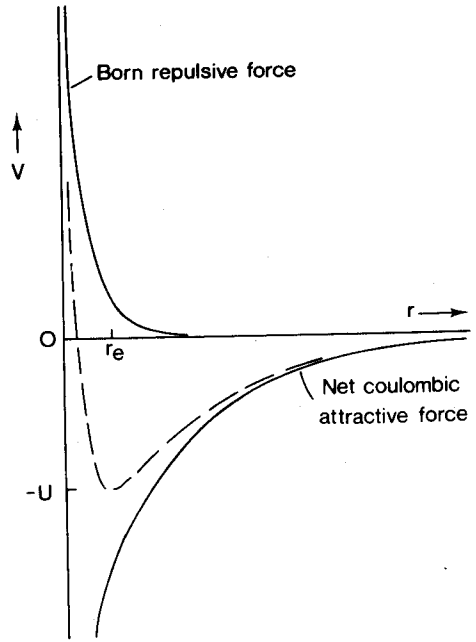

Fig. 8.5 Lattice energy (dashed line) of ionic crystals as a function of internuclear separation

then

$$B = \frac{e^2 Z_+ Z_- A r^{n-1}}{n} \tag{8.16}$$

and therefore

$$U = -\frac{e^2 Z_+ Z_- NA}{r_e}\left(1 - \frac{1}{n}\right) \tag{8.17}$$

The dashed line in Fig. 8.5 shows schematically the variation of U with r and gives the minimum U value when $r = r_e$.

For most practical purposes, equation (8.17) is entirely satisfactory, but in more refined treatments certain modifications are made:

(a) The Born repulsive energy term is better represented by an exponential function:

$$V = B\exp\left(\frac{-r}{\rho}\right) \tag{8.18}$$

where ρ is a constant, typically 0.35. When r is small ($r \ll r_e$), equations (8.8) and (8.18) give very different values for V, but for realistic interatomic distances, i.e. $r \simeq r_e$, the two values are similar. Use of equation (8.18) in the

expression for U gives the *Born–Mayer equation*:

$$U = -\frac{e^2 Z_+ Z_- AN}{r_e}\left(1 - \frac{\rho}{r_e}\right) \tag{8.19}$$

(b) The zero point energy of the crystal should be included in the calculation of U. This is equal to $2.25\,h\nu_{O_{max}}$, where $\nu_{O_{max}}$ is the frequency of the highest occupied vibrational mode in the crystal. Its inclusion leads to a small reduction in U.

(c) Van der Waals attractive forces exist between ions due to induced dipole–induced dipole interactions between them. These are of the form NC/r^6 and lead to an increase in U.

A more complete equation for U, after correcting for these factors, is

$$U = -\frac{Ae^2 Z_+ Z_- N}{r} + BNe^{-r/\rho} - CNr^{-6} + 2.25Nh\nu_{O_{max}} \tag{8.20}$$

Typical values for these four terms, in kilojoules per mole, are (from Greenwood):

Substance	$NAe^2Z_+Z_-r^{-1}$	$NBe^{-r/\rho}$	NCr^{-6}	$2.25Nh\nu_{O_{max}}$	U
NaCl	− 859.4	98.6	− 12.1	7.1	− 765.8
MgO	− 4631	698	− 6.3	18.4	− 3921

from which it can be seen that the Born repulsive term contributes 10 to 15 per cent to the value of U whereas the zero point vibrational and van der Waals terms contribute about 1 per cent each and, being of opposite sign, tend to cancel each other out. For most purposes, therefore, we can use the simplified equation (8.17); let us consider each of the terms in equation (8.17) and evaluate their significance.

The magnitude of U depends on six parameters A, N, e, Z, n and r_e, four of which are constants for a particular ionic structure type. This leaves just two variables, the charge on the ions, Z_+, Z_-, and the internuclear separation, r_e. Of the two, the charge is by far the most important since the value of the product (Z_+Z_-) is capable of much larger variation than is r_e. For instance, a material with divalent ions should have a lattice energy that is four times as large as an isostructural crystal with the same r_e but containing monovalent ions (compare alkaline earth oxides and alkali halides, in the above table). For a series of isostructural phases with the same Z values but increasing r_e, a decrease in U is expected (e.g. alkali fluorides, alkaline earth oxides with NaCl structure). A selection of lattice energies for materials with the rock salt structure and showing these two trends is given in Table 8.6.

Since the lattice energy of a crystal is equivalent to its heat of dissociation, a correlation exists between U and the melting point of the crystal (a better

Table 8.6 *Some lattice energies (kJ mol^{-1}).* (Data from Ladd and Lee, 1963)

MgO	3938	LiF	1024	NaF	911
CaO	3566	LiCl	861	KF	815
SrO	3369	LiBr	803	RbF	777
BaO	3202	LiI	744	CsF	748

correlation may be sought between U and the sublimation energy, but such data are rarely available). The effect of (Z_+Z_-) on the melting point is shown by the refractoriness of the alkaline earth oxides (m.p. of CaO = 2572 °C) compared with the alkali halides (m.p. of NaCl = 800 °C). The effect of r_e on melting points may be seen in series such as:

MgO(2800 °C), CaO(2572 °C) and BaO(1923 °C)

8.2.6 Kapustinskii's equation

Kapustinskii (1956) noted an empirical increase in the value of the Madelung constant, A, as the coordination number of the ions in the structure increased, e.g. in the series ZnS, NaCl, CsCl (Table 8.5). Since, for a particular anion and cation, r_e also increases with coordination number (e.g. Fig. 8.3), Kapustinskii proposed a general equation for U in which variations in A and r_e are auto-compensated. He suggested using the rock salt value for A and octahedral ionic radii (Goldschmidt) in calculating r_e; substituting $r_e = r_c + r_a$, $\rho = 0.345$, $A = 1.745$ and values for N and e into equation (8.19) gives the Kapustinskii equation:

$$U = \frac{1200.5 V Z_+ Z_-}{r_c + r_a}\left(1 - \frac{0.345}{r_c + r_a}\right) \quad \text{kJ mol}^{-1} \qquad (8.21)$$

where V is the number of ions per formula unit (two in NaCl, three in PbF_2, etc.). This formula may be used to calculate the lattice energy of any known or hypothetical ionic compound and in spite of the assumptions involved, the answers obtained are surprisingly accurate.

The Kapustinskii equation has been used to successfully predict the stable existence of several previously unknown compounds. In cases where U is known from Born–Haber cycle calculations (see later), it has been used to derive values for ionic radii. This has been particularly useful for complex anions, e.g. SO_4^{2-}, PO_4^{3-}, whose effective size in crystals is difficult to measure by other means.

Table 8.7 *Thermochemical radii* (Å) *of complex anions.* (Data from Kapustinskii, 1956)

BF_4^-	2.28	CrO_4^{2-}	2.40	IO_4^-	2.49
SO_4^{2-}	2.30	MnO_4^-	2.40	MoO_4^{2-}	2.54
ClO_4^-	2.36	BeF_4^-	2.45	SbO_4^{3-}	2.60
PO_4^{3-}	2.38	AsO_4^{3-}	2.48	BiO_4^{3-}	2.68
OH^-	1.40	O_2^{2-}	1.80	CO_3^{2-}	1.85
NO_2^-	1.55	CN^-	1.82	NO_3^-	1.89

Radii determined in this way are known as *thermochemical radii* and some values are given in Table 8.7. It should be noted that radii for non-spherical ions such as CN^- represent gross simplifications and are only really applicable to other lattice energy calculations.

8.2.7 The Born–Haber cycle and thermochemical calculations

The lattice energy of a crystal is equivalent to its heat of formation from one mole of its ionic constituents in the gas phase:

$$Na^+(g) + Cl^-(g) \rightarrow NaCl(s), \qquad \Delta H = U$$

It cannot be measured experimentally. However, the heat of formation of a crystal, ΔH_f, can be measured relative to the reagents in their standard states:

$$Na(s) + \tfrac{1}{2}Cl_2(g) \rightarrow NaCl(s), \qquad \Delta H = \Delta H_f$$

ΔH_f may be related to U by constructing a thermochemical cycle known as a Born–Haber cycle, in which ΔH_f is given by the summation of energy terms in a hypothetical reaction pathway. For NaCl, the individual steps in the pathway, commencing with the elements in their standard states, are:

Sublimation of solid Na	$\Delta H = S$
Ionization of gaseous Na atoms	$\Delta H = \text{IP}$
Dissociation of Cl_2 molecules	$\Delta H = \frac{1}{2}D$
Formation of the Cl^- ion	$\Delta H = \text{EA}$
Coalescence of gaseous ions to give crystalline NaCl	$\Delta H = U$

Addition of these five terms is equivalent to forming crystalline NaCl from solid Na and Cl_2 molecules, as shown:

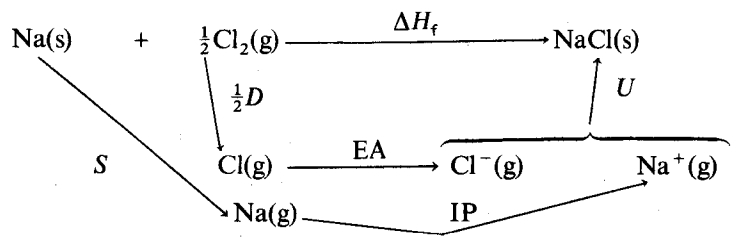

From Hess' Law,

$$\Delta H_f = S + \tfrac{1}{2}D + \text{IP} + \text{EA} + U \qquad (8.22)$$

Applications. The Born–Haber cycle and equation (8.22) have various uses:

(a) Six enthalpy terms are present in equation (8.22). If all six can be determined independently for a particular compound, then the cycle gives a check on the

internal consistency of the data. The values for NaCl are as follows:

S	$109\ kJ\ mol^{-1}$
IP	$493.7\ kJ\ mol^{-1}$
$\frac{1}{2}D$	$121\ kJ\ mol^{-1}$
EA	$-356\ kJ\ mol^{-1}$
U	$-764.4\ kJ\ mol^{-1}$
ΔH_f	$-410.9\ kJ\ mol^{-1}$

Summation of the first five terms gives a calculated H_f of $-396.7\ kJ\ mol^{-1}$, which compares reasonably well with the measured ΔH_f value of $-410.9\ kJ\ mol^{-1}$.

(b) If only five of the energy terms are known, then the sixth may be evaluated using equation (8.22). An early application ($\sim$ 1918) was in the calculation of electron affinities, for which data were not then available.

(c) The possible stability of an unknown compound may be estimated. It is necessary to assume a structure for the compound in order to calculate U and while there are obviously errors involved, e.g. in choosing r_e, these are usually unimportant compared with the effect of some of the other energy terms involved in equation (8.22). Having estimated U, ΔH_f may then be calculated. If ΔH_f is large and positive then this explains why the compound is unknown—it is unstable relative to its elements. If ΔH_f(calc.) is negative, however, it may be worth while to try and prepare the compound under certain conditions. Examples are given in Section 8.2.8.

(d) Differences between values of lattice energies obtained by the Born–Haber cycle using thermochemical data and theoretical values calculated from an ionic model of the crystal structure may be used as evidence for non-ionic bonding effects. Data for the silver halides (Table 8.8) and for thallium and copper halides (not given) show that the differences between the two lattice energies are least for the fluorides and greatest for the iodides. This is attributed to the presence of a strong covalent contribution to the bonding in the iodides which leads to an increase in the values of the thermochemical lattice energy. A correlation also exists between the insolubility of the Ag salts, especially AgI, in water and the presence of partial covalent bonding. Data for the corresponding alkali halides show that the differences between thermochemical and calculated lattice energies are small and indicate that the ionic bonding model may be applied satisfactorily to them.

While covalent bonding is present in, for example, AgCl and AgBr, as evidenced by the lattice energies, it is not strong enough to change the crystal structure from that of rock salt to one of lower coordination number. AgI does have a different structure, however; it is polymorphic and can exist in at least three structure types, all of which have low coordination numbers, usually four. Changes in structure type and coordination number due to increased covalent bonding are described in Section 8.1.2.

Table 8.8 *Lattice energies ($kJ\ mol^{-1}$) of some Group I halides.* (Data from Waddington, 1959)

	U_{calc}	$U_{Born-Haber}$	ΔU
AgF	920	953	33
AgCl	832	903	71
AgBr	815	895	80
AgI	777	882	105

(e) Certain transition metals have crystal field stabilization energies due to their d electron configuration (Section 8.6.1.1) and this gives an increased lattice energy in their compounds. For example, the difference between experimental and calculated lattice energies in CoF_2 is $83\ kJ\ mol^{-1}$, which is in fair agreement with the CFSE value calculated for the high spin state of Co in CoF_2 of $104\ kJ\ mol^{-1}$. Ions which do not exhibit CFSE effects are those with configurations d^0 (e.g. Ca^{2+}), d^5 high spin (e.g. Mn^{2+}) and d^{10} (e.g. Zn^{2+}). A further discussion is given in Section 8.6.1.1.

(f) The Born–Haber cycle has many other uses, e.g. in solution chemistry to determine energies of complexation and hydration of ions. These usually require a knowledge of the lattice energy of the appropriate solids, but since these applications do not provide any new information about solids, they are not discussed further.

8.2.8 Stabilities of real and hypothetical compounds

8.2.8.1 *Inert gas compounds*

One may ask, is it worth while trying to synthesize, for example, ArCl? Apart from ΔH_f, the only unknown in equation (8.22) is U. Suppose that hypothetical ArCl had the rock salt structure and the radius of the Ar^+ ion is between that of Na^+ and K^+. An estimated lattice energy for ArCl is, then, $-745\ kJ\ mol^{-1}$ (NaCl = −764.4; KCl = −701.4). Substitution in equation (8.22) gives, in kilojoules per mole:

S	$\frac{1}{2}D$	IP	EA	U	ΔH_f(calc.)
0	121	1524	−356	−745	+544

from which it can be seen that ArCl has a large positive heat of formation and would be thermodynamically unstable, by a large amount, relative to the elements.

Such a calculation also tells us *why* ArCl is unstable and cannot be synthesized. Comparing the calculations for ArCl and NaCl, it is clear that the instability of ArCl is due to the very high ionization potential of argon (stability is strictly governed by free energies of formation, but ΔS is small and hence $\Delta G \simeq \Delta H$). The heats of formation calculated for several other hypothetical compounds are given in Table 8.9.

Table 8.9 *Enthalpies of formation ($kJ\ mol^{-1}$) of some hypothetical (*) and real compounds*

HeF*	+1066	NeCl*	+1028	$CsCl_2^*$	+213	CuI_2	−21
ArF*	+418	NaCl	−411	CsF_2^*	−125	$CuBr_2$	−142
XeF*	+163	MgCl*	−125	AgI_2^*	+280	$CuCl_2$	−217
$MgCl_2$	−639	AlCl*	−188	$AgCl_2$	+96	CuF_2	−890
$NaCl_2^*$	+2144	$AlCl_3$	−694	AgF_2	−205		

There is now a large number of inert gas compounds known, following on from the preparation of $XePtF_6$ by Bartlett in 1962. Consideration of lattice energies and enthalpies of formation led Bartlett to try and synthesize $XePtF_6$ by direct reaction of Xe and PtF_6 gases. He had previously prepared O_2PtF_6 as an ionic salt, $(O_2)^+(PtF_6)^-$, by reacting (by accident) O_2 with PtF_6. From a knowledge of the similarity in the first ionization potentials of molecular oxygen ($1176\ kJ\ mol^{-1}$) and xenon ($1169\ kJ\ mol^{-1}$), he reasoned, correctly, that the corresponding xenon compound should be stable.

8.2.8.2. *Lower and higher valence compounds*

Consider alkaline earth compounds. In these, the metal is always divalent. Since a great deal of extra energy is required to doubly ionize the metal atoms, it is reasonable to ask why monovalent compounds, such as MgCl, do not form. Data in Table 8.9 show that MgCl is indeed stable relative to the elements (ΔH(calc.) = $-125\ kJ\ mol^{-1}$) but that $MgCl_2$ is much more stable ($\Delta H = -639\ kJ\ mol^{-1}$). This is shown by the following sequence:

$$2Mg + Cl_2 \xrightarrow{-250} 2MgCl \xrightarrow{-389} Mg + MgCl_2$$
$$2Mg + Cl_2 \xrightarrow{\qquad -639 \qquad} Mg + MgCl_2$$

In any attempt to synthesize MgCl, attention should be directed towards keeping the reaction temperature low and/or isolating the MgCl product, in order to prevent it from reacting further or disproportionating. Similar trends are observed for other hypothetical compounds such as ZnCl, Zn_2O, AlCl and $AlCl_2$.

From a consideration of the factors that affect the stability of compounds, the following conclusions may be drawn about compounds with metals in unusual oxidation states:

(a) The formation and stability of compounds with lower than normal valence states appears to be favourable when (i) the second, and higher, ionization potentials of the metal are particularly high and (ii) the lattice energy of the corresponding compounds with the metal in its normal oxidation state is reduced.

(b) Conversely, in order to prepare compounds in which the metal has a higher than normal oxidation state and in which it is probably necessary to break into a closed electron shell, it is desirable to have (i) low values for the second (or higher) ionization potential of the metal atoms and (ii) large lattice energies of the resulting higher valence compounds.

As examples of these trends, calculations for the alkaline earth monohalides show that while all are unstable relative to the dihalides, the enthalpy of disproportionation is least in each case for the iodide ($U_{(MI_2)} < U_{(MBr_2)}$, etc.—effect a, ii). Higher valence halogen compounds of the Group I elements are most likely to occur with caesium and the copper subgroup elements (effect b, i), in combination with fluorine (effect b, ii). Thus, from Table 8.9, all caesium dihalides, apart from CsF_2, have positive ΔH_f values and would be unstable. CsF_2 is stable in principle, with its negative ΔH_f value, but has not been prepared because its disproportionation to CsF has a large negative ΔH:

$$Cs + F_2 \xrightarrow{-125} CsF_2 \xrightarrow{-405} CsF + \tfrac{1}{2}F_2$$
$$Cs + F_2 \xrightarrow{\qquad -530 \qquad} CsF + \tfrac{1}{2}F_2$$

For the silver dihalides, ΔH_f becomes less positive and finally negative across the series AgI_2 to AgF_2. This again shows the effect of r_e on U and hence on ΔH_f (effect b, ii). Unlike CsF_2, AgF_2 is a stable compound since AgF and AgF_2 have similar enthalpies of formation and therefore the disproportionation enthalpy of AgF_2 (to $AgF + \frac{1}{2}F_2$) is ~zero.

The copper halides are particularly interesting. The divalent state of copper, in which the d^{10} shell of copper is broken into, is the most common state and again the dihalides show decreasing stability across the series CuF_2 to CuI_2 (Table 8.9): CuI_2 appears not to exist and its calculated ΔH_f is barely negative. On the other hand, in the monovalent state the situation is reversed and all the halides apart from CuF are known. CuF is calculated to be stable relative to the elements but not relative to CuF_2:

$$2Cu + F_2 \xrightarrow{-36} 2CuF \xrightarrow{-91} CuF_2 + Cu$$
$$2Cu + F_2 \xrightarrow{\qquad -127 \qquad} CuF_2 + Cu$$

The above examples show that several factors affect the formulae and stability of compounds: ionization potentials, lattice energies (via internuclear distances and the charges on ions) and the relative stability of elements in different oxidation states. Often a delicate balance between opposing factors controls the stability or instability of a compound and, as with the copper halides, detailed calculations are needed to assess the factors involved.

8.2.9 Polarization and partial covalent bonding

Covalent bonding, partial or complete, occurs when the outer electronic charge density on an anion is polarized towards and by a neighbouring cation. The net effect is that an electron pair which would be associated entirely with the anion in a purely ionic structure is displaced to occur between the anion and cation such that the electron pair is common to both. In cases of partial covalent bonding, some of the electron density is common to both atoms but the rest is still associated with the more electronegative atom.

The occurrence of partial covalent bonding in an otherwise ionic structure may

sometimes be detected by abnormally large values of the lattice energy (Section 8.2.7). In other cases, it is clear from the nature of the structure and the coordination numbers of the atoms that the bonding cannot be purely ionic (Section 8.1.2). Until comparatively recently, it has been difficult to quantify the degree of partial covalence in a particular structure, although one has intuitively felt that most so-called, ionic structures must have a considerable degree of covalent character. Two new approaches which have had considerable success are the coordinated polymeric model of Sanderson and the ionicity plots of Mooser and Pearson.

8.3 Coordinated polymeric structures—Sanderson's model

A fresh approach to the theory and description of non-molecular crystal structures has been developed by Sanderson (1967, 1976). Basically, he regards all bonds in non-molecular crystal structures as being polar covalent. The atoms contain partial charges whose values may be calculated readily using a new scale of electronegativities developed by Sanderson. From the partial charges, the relative contributions of ionic and covalent bonding to the total bond energy may be estimated. Since all non-molecular crystals contain only partially charged atoms, the ionic model represents an extreme form of bonding that is not attained in practice. Thus in, for example, KCl, the charges on the atoms are calculated to be ± 0.76 instead of ± 1.0 for a purely ionic structure.

The essential features of this new approach to non-molecular solids, which is part of a more general and widely applicable theory of bonding, are as follows. The features of an atom which control its physical and chemical properties are (a) its electronic configuration and (b) the effective nuclear charge felt by the valence electrons. It is recognition of the importance of the latter effect that provides the starting point for Sanderson's theory.

8.3.1 Effective nuclear charge

The *effective nuclear charge* of an atom is the positive charge that would be felt by a foreign electron on arriving at the periphery of the atom. Atoms are, of course, electrically neutral overall but, nevertheless, the valence electrons of an atom are not very effective in shielding the outside world from the positive charge on the nucleus of the atom. Consequently, an incoming electron (e.g. an electron that belongs to a neighbouring atom and is coming to investigate the possibility of bond formation) feels a positive, attractive charge. Were this not the case and the surface of an atom was completely shielded from the nuclear charge, then atoms would have zero electron affinity and no bonds, ionic or covalent, would ever form.

The effective nuclear charge is greatest in elements which have a single vacancy in their valence shell, i.e. in the halogens. In the inert gases, the outermost electron shell is full and no foreign electrons can enter it. Consequently, incoming electrons would have to occupy vacant orbitals which are essentially 'outside' the

atom and the effective nuclear charge experienced in such orbitals would be greatly reduced. Calculations of 'screening constants' were made by Slater who found that outermost electrons are much less efficient at screening nuclear charge than are electrons in inner shells. The screening constants of outermost electrons are calculated to be approximately one third; this means that for each unit increase in atomic number and positive nuclear charge across the series, e.g. sodium to chlorine, the additional positive charge is screened by only one third. Therefore, the effective nuclear charge increases in steps of two thirds and the valence electrons experience an increasingly strong attraction to the nucleus on going from sodium to chlorine. Similar effects occur throughout the periodic table: the effective nuclear charge is small for the alkali metals and increases to a maximum in the halogens.

Many atomic properties may be correlated with effective nuclear charge:

(a) Ionization potentials gradually increase from left to right across the periodic table.
(b) Electron affinites become increasingly negative in the same direction.
(c) Atomic radii progressively decrease from left to right.
(d) Electronegativities increase from left to right.

Let us consider two of these properties, atomic radii and electronegativities, in more detail.

8.3.2 Atomic radii

Atomic radii vary considerably for a particular atom depending on bond type and coordination number and many tabulations of radii are available; indeed, the subject of ionic radii is still a controversial subject. Fortunately, however, the *non-polar covalent radii* of atoms can be measured accurately and represent a point of reference with which to compare other radii. Thus the atomic, non-polar covalent radius of carbon, given by half the C—C single bond length is constant at 0.77 Å in materials as diverse as diamond and gaseous, paraffin hydrocarbons. Non-polar radii of atoms are listed in Table 8.10; from these radii, it is possible, using Sanderson's method, to estimate the effect that partial charges on atoms have on their radii. The general trends are that with increasing amounts of partial positive charge, the radii become smaller (i.e. as electrons are removed from the valence shell, but with the nuclear charge unchanged, so the remaining valence shell electrons feel a stronger attraction to the nucleus and the atom contracts). Conversely, with increasing negative charge on the atom, the radius becomes larger. Sanderson developed a simple, empirical formula to quantify the variation of radius, r, with partial charge:

$$r = r_c - B\delta \tag{8.23}$$

where r_c is the non-polar covalent radius, B is a constant for a particular atom and δ is its partial charge. B values are also given in Table 8.10. The partial

Table 8.10 *Some electronegativity and size parameters of atoms. (After Sanderson, 1976)*

Element	S	r_c(Å)	B(solid)	ΔS_c	r_i(Å)
H	3.55	0.32		3.92	
Li	0.74	1.34	0.812	1.77	0.53
Be	1.99	0.91	0.330	2.93	0.58
B	2.93	0.82		2.56	
C	3.79	0.77		4.05	
N	4.49	0.74		4.41	
O	5.21	0.70	4.401	4.75	1.10
F	5.75	0.68	0.925	4.99	1.61
Na	0.70	1.54	0.763	1.74	0.78
Mg	1.56	1.38	0.349	2.60	1.03
Al	2.22	1.26		3.10	
Si	2.84	1.17		3.51	
P	3.43	1.10		3.85	
S	4.12	1.04	0.657	4.22	1.70
Cl	4.93	0.99	1.191	4.62	2.18
K	0.42	1.96	0.956	1.35	1.00
Ca	1.22	1.74	0.550	2.30	1.19
Zn	2.98			3.58	
Ga	3.28			3.77	
Ge	3.59	1.22		3.94	
As	3.90	1.19		4.11	
Se	4.21	1.16	0.665	4.27	1.83
Br	4.53	1.14	1.242	4.43	2.38
Rb	0.36	2.16	1.039	1.25	1.12
Sr	1.06	1.91	0.429	2.14	1.48
Ag	2.59	1.50	0.208		1.29
Cd	2.84	1.46	0.132	3.35	1.33
Sn	3.09	1.40		3.16, 3.66	
Sb	3.34	1.38		3.80	
Te	3.59	1.35	0.692	3.94	2.04
I	3.84	1.33	1.384	4.08	2.71
Cs	0.28	2.35	0.963	1.10	1.39
Ba	0.78	1.98	0.348	1.93	1.63
Hg	2.93			3.59	
Tl	3.02	1.48		2.85	
Pb	3.08	1.47		3.21, 3.69	
Bi	3.16	1.46		3.74	

charges on atoms cannot be measured directly but may be estimated from Sanderson's electronegativity scale, as follows.

8.3.3 Electronegativity and partially charged atoms

The electronegativity of an atom is a measure of the net attractive force experienced by an outermost electron interacting with the nucleus (Gordy, Allred and Rochow). The concept of electronegativity was originated by Pauling as a

parameter that would correlate with the observed polarity of bonds between unlike atoms. Atoms of high electronegativity attract electrons (in a covalent bond) more than do atoms of low electronegativity and, hence, they acquire a partial negative charge. The magnitude of the partial charge depends on the initial difference in electronegativity between the two atoms. The difficulty in working with electronegativities in the past has been that electronegativity has not had a precise definition and, therefore, it has not been possible to use an absolute scale of electronegativities and make accurate calculations. Pauling observed a correlation between the strengths of polar bonds and the degree of polarity in the bonds. He proposed that bond strengths are a combination of (a) a homopolar bond energy and (b) an 'extra ionic energy' due to bond polarity and, hence, electronegativity difference. He then used this correlation between polarity and extra ionic energy to establish his scale of electronegativities. These ideas have since been extended and modified by Sanderson to permit quantitative calculations of bond energies to be made for a wide variety of compounds. However, Sanderson used a different method to derive a scale of electronegativities. Since electronegativity is a measure of the attractive force between the effective nuclear charge and an outermost electron, it is related to the compactness of an atom. He used the relation:

$$S = \frac{D}{D_a} \tag{8.24}$$

to evaluate the electronegativity, S, in which D is the electron density of the atom (given by the ratio of atomic number: atomic volume) and D_a is the electron density that would be expected for the atom by linear interpolation of the D values for the inert gas elements. The electronegativity values so obtained are listed in Table 8.10, with some minor modifications made by Sanderson.

An important contribution to our understanding of bond formation is *the principle of electronegativity equalization* proposed by Sanderson. It may be stated: 'When two or more atoms initially different in electronegativity combine chemically, they become adjusted to the same intermediate electronegativity within the compound.' It is found in practice that the value of the intermediate electronegativity is given by the geometric mean of the individual electronegativities of the component atoms, e.g. for NaF:

$$S_b = \sqrt{S_{Na} S_F} = 2.006 \tag{8.25}$$

This means that in a bond between unlike atoms, the bonding electrons are preferentially and partially transferred from the less electronegative to the more electronegative atom. A partial negative charge on the more electronegative atom results whose magnitude is defined, by Sanderson, as follows: '*Partial charge* is defined as the ratio of the change in electronegativity undergone by an atom on bond formation to the change it would have undergone on becoming completely ionic with charge + or − 1.'

In order to make calculations of partial charges, a point of reference was necessary and for this it was assumed that the bonds in NaF are 75 per cent ionic;

this assumption appears to have been well justified by subsequent developments. Further, it was necessary to assume that electronegativity changes linearly with charge. It can then be shown that the change in electronegativity, ΔS_c, of any atom on acquiring a unit positive or unit negative charge is given by

$$\Delta S_c = 2.08\sqrt{S} \tag{8.26}$$

Partial charge, δ, may therefore be defined as

$$\delta = \frac{\Delta S}{\Delta S_c} \tag{8.27}$$

where $\Delta S = S - S_b$. Values of ΔS_c are also given in Table 8.10.

Returning now to the radii of partially charged atoms, the problem in assigning individual radii to atoms or ions has been the question of how to divide an experimentally observed internuclear distance into its component radii. Many methods have been tried and various tabulations of radii are available. All of them are additive in that they correctly predict bond distances. The method adopted by Pauling (and Sanderson) has been to divide the experimental internuclear distance in an isoelectronic 'ionic' crystal, such as NaF, according to the inverse ratio of the effective nuclear charges on the two 'ions'. The effective nuclear charges can be calculated from the screening constants. From a knowledge of the partial charges on the atoms and assuming that radii change systematically with partial charge (according to the relation $r = r_c - B\delta$), the ionic radii of Na^+ and F^- may be calculated; these then serve as a point of reference for calculating radii of other ions in materials that are not isoelectronic. In Table 8.10 are listed the radii of singly charged ions in the solid state calculated by the above method; also given are B and r_c data to enable the radii of partially charged atoms to be calculated and electronegativity data S, ΔS_c to enable the partial charges, δ, to be calculated.

Let us consider the use of these data for one example, BaI_2. From Table 8.10, $S_{Ba} = 0.78$ and $S_I = 3.84$; the intermediate electronegativity, S_b, is given by $S_b = \sqrt[3]{S_{Ba}S_I^2} = 2.26$. Therefore, for barium, $\Delta S = 2.26 - 0.78 = 1.48$ and for iodine, $\Delta S = 3.84 - 2.26 = 1.58$. The values of ΔS_c are 1.93 (Ba) and 4.08(I). Hence $\delta_{Ba} = 1.48/1.93 = 0.78$ and $\delta_I = 1.58/4.08 = -0.39$, i.e. BaI_2 is ~39 per cent ionic, 61 per cent covalent (using the δ_I value). The radii of the partially charged atoms may now be calculated. For barium, $r_c = 1.98$, $B = 0.348$ and δ is calculated to be 0.78; hence $r_{Ba} = r_c - B\delta = 1.71$ Å. For iodine, $r_c = 1.33$, $B = 1.384$ and $\delta = -0.39$; hence $r_I = 1.87$ Å. Therefore, the barium–iodine distance is calculated to be $1.87 + 1.71 = 3.58$ Å, which compares very well with the experimental value of 3.59 Å.

Using the above methods, Sanderson has evaluated the partial charges and atomic radii in a large number of solid compounds. For example, data are given in Table 8.11 for a number of mono- and divalent chlorides; the charge on the chloride atom varies from -0.21 in $CdCl_2$ to -0.81 in CsCl and at the same time the calculated radius of the chlorine atom varies from 1.24 to 1.95 Å. These

Table 8.11 *Partial charge and radius of the chlorine atom in some solid chlorides*

Compound	$-\delta_{Cl}$	r_{Cl}(Å)
$CdCl_2$	0.21	1.24
$BeCl_2$	0.28	1.26
CuCl	0.29	1.34
AgCl	0.30	1.35
$MgCl_2$	0.34	1.39
$CaCl_2$	0.40	1.47
$SrCl_2$	0.43	1.50
$BaCl_2$	0.49	1.57
LiCl	0.65	1.76
NaCl	0.67	1.79
KCl	0.76	1.90
RbCl	0.78	1.92
CsCl	0.81	1.95

compare with a non-polar covalent radius of 0.99 Å and an ionic radius of 2.18 Å (Table 8.10). While these radii and partial charges may not be quantitatively correct, because some of the assumptions involved in their calculation are rather empirical, they nevertheless appear to be realistic. Most of the compounds in Table 8.11 are normally regarded as ionic, and if the data are in any way correct, they clearly show that it is unrealistic and misleading to assign a radius to the chloride ion which is constant for all solid chlorides.

A similar but more extensive list of the partial charge on oxygen in a variety of oxides in given in Table 8.12, where values cover almost the entire range between 0 and -1. Although oxides are traditionally regarded as containing the oxide

Table 8.12 *Partial charge on oxygen in some solid oxides*

Compound	$-\delta_O$	Compound	$-\delta_O$	Compound	$-\delta_O$	Compound	$-\delta_O$
Cu_2O	0.41	HgO	0.27	Ga_2O_3	0.19	CO_2	0.11
Ag_2O	0.41	ZnO	0.29	Tl_2O_3	0.21	GeO_2	0.13
Li_2O	0.80	CdO	0.32	In_2O_3	0.23	SnO_2	0.17
Na_2O	0.81	CuO	0.32	B_2O_3	0.24	PbO_2	0.18
K_2O	0.89	BeO	0.36	Al_2O_3	0.31	SiO_2	0.23
Rb_2O	0.92	PbO	0.36	Fe_2O_3	0.33	MnO_2	0.29
Cs_2O	0.94	SnO	0.37	Cr_2O_3	0.37	TiO_2	0.39
		FeO	0.40	Sc_2O_3	0.47	ZrO_2	0.44
		CoO	0.40	Y_2O_3	0.52	HfO_2	0.45
		NiO	0.40	La_2O_3	0.56		
		MnO	0.41				
		MgO	0.50				
		CaO	0.56				
		SrO	0.60				
		BaO	0,68				

ion, O^{2-}, the calculations show that the actual charge carried by an oxygen never exceeds -1 and is usually much less than -1.

These ideas and calculations on partial charges which have been developed by Sanderson enable many correlations to be made between partial charge and chemical properties. To give one example, the acidic, amphoteric and basic properties of oxides correlate nicely with the partial charge on the oxide ion and the changeover in behaviour occurs with a partial charge of ~ -0.30. We are concerned here, however, with the structures of solids. Since the ionic model appears to be inappropriate or only partially correct for most solids, Sanderson proposed the *coordinated polymeric model* for solids. This is essentially a blend of the two extreme forms of bonding: ionic and covalent.

8.3.4 Coordinated polymeric structures

From the principle of electronegativity equalization, electrons in a hypothetical covalent bond are partially transferred to the more electronegative atom. This removal of electrons from the electropositive atom leads to an increase in its effective nuclear charge, decrease in its size and hence an increase in its effective electronegativity. Likewise, as the electronegative atom acquires electrons, so its ability to attract still more electrons diminishes and its electronegativity decreases. In this way the electronegativities of the two atoms adjust themselves until they are equal. This principle of electronegativity equalization may be applied equally to diatomic gas molecules, in which only one bond is involved, or to three-dimensional solid structures in which each atom is surrounded by and bonded to several others. This argument illustrates how covalent bonds that are initially non-polar may become polar due to the electronegativity equalization. An alternative approach is to start with purely ionic bonding and consider how the bonds may acquire some covalent character. In an ionic structure, M^+X^-, the cations are surrounded by anions (usually 4, 6 or 8). However, the cations have empty valence shells and are potential electron pair acceptors; likewise, anions with their filled valence shells are potential electron pair donors. The cations and anions therefore interact in the same way as do Lewis acids and bases: the anions, with their lone pairs of electrons, coordinate to the surrounding cations. The strength of this interaction, and hence the degree of covalent bonding which results, is again related to the electronegativities of the two atoms. Thus electronegative cations such as Al^{3+} are much stronger electron pair acceptors (and Lewis acids) than are electropositive cations such as K^+. The coordinated polymeric model of structures proposed by Sanderson is based on this idea of acid–base interactions between ions. It therefore forms a bridge between the ionic and covalent extremes of bond type.

8.3.5 Bond energy calculations

In most solids, the bonds are a blend of covalent and ionic. For simplicity and convenience in calculations, it is possible to regard the bonds as being wholly ionic for part of the time and wholly covalent for the remainder of the time. The relative proportions of the two components are then directly related to the partial charges on the atoms. In Pauling's view of polar bonds, the ionic contribution to the bond energy, due to the electronegativity difference between the atoms, is regarded as *adding to* the energy of a 100 per cent covalent bond. However, Sanderson argues that the ionic contribution *replaces* part of the covalent contribution; since ionic bonds always have higher energy than covalent bonds this automatically leads to an increasing bond energy with increasing bond polarity.

The ionic contribution to bond energy may be calculated using the Born–Mayer equation (8.19) of Section 8.2.5; the lattice energy for a purely ionic crystal is calculated in this way and multiplied by the fractional ionic character of the bonds. Covalent bond energies are estimated as follows.

For a homopolar, covalent bond between like atoms, Sanderson proposed the relation:

$$E = CrS \tag{8.28}$$

between the covalent bond energy, E, the electronegativity, S, and non-polar covalent radius, r, of the atoms; C is an empirical constant. The value of C is the same across, for example, the series, Li...F, for which a plot of E against (rS) is shown in Fig. 8.6. The linearity of the plot was shown by the experimental data for Li, Be, B and C; these values were obtained from the dissociation energies of gas phase molecules such as Li_2. By extrapolation, single bond energies of N, O and F were then estimated. It is known that the experimentally determined single bond energies of these atoms, N, O and F, are anomalous, e.g. the F_2 bond

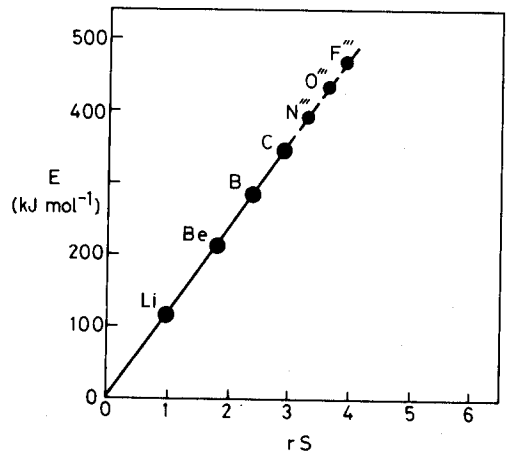

Fig. 8.6 Plot of homopolar bond energy, E, against rS, the product of non-polar covalent radius, r, and Sanderson electronegativity, S. E values for N, O and F are obtained by extrapolation

dissociation energy is much less than expected by comparison with the values for the other halogens. The experimental bond dissociation energies for O, N and F are reduced by what Sanderson calls the 'lone pair bond weakening effect' (Section 8.3.6).

From Fig. 8.6 it is possible to estimate bond energies for these elements which would be free from the lone pair bond weakening effect. Thus the value for fluorine, F‴, extrapolated from Fig. 8.6 is 466 kJ mol^{-1} whereas the experimental value obtained from the dissociation of the F_2 molecule is only 165 kJ mol^{-1}. Using a similar procedure, single covalent bond energies have been estimated for most of the main group elements in cases where such data were not already available.

The next step is to calculate the covalent bond energy, E_c of a heteronuclear bond. Sanderson used Pauling's equation, but added a correction factor for bond length: for a bond between atoms A and B, in a molecule,

$$E_c = \frac{R_c}{R_o}\sqrt{E_{AA}E_{BB}} \tag{8.29}$$

i.e. the bond energy is the geometric mean of the two homonuclear bond energies, E_{AA} and E_{BB}, multiplied by the ratio R_c/R_o in which R_c is the sum of the covalent radii (tabulated) and R_o is the observed bond length.

For crystalline solids, a correction factor is needed for the total number of electron pairs, n, that are involved in the bonding. Thus, in gaseous NaCl molecules, there is only one electron pair and one bond to be considered, whereas in crystalline NaCl each atom is coordinated to six others and, on the coordinated polymeric model of bonding, there are four electron pairs to be distributed over the six bonds around any particular atom. For most solid oxides and halides on which calculations have been made, use of $n = 4$ gives good agreement between experimental and calculated bond energies. In some cases, especially with the smaller atoms, and for reasons which are not understood, it appears necessary to use $n = 3$ and occasionally $n = 6$.

The total bond energy, E, of a crystalline solid is given by the sum of the ionic and covalent contributions, i.e.

$$E = t_c E_c n + \frac{t_i U}{f} \tag{8.30}$$

where t_c and t_i are the fractional covalent and ionic characters, respectively, in the bonds. The term U/f is a modified lattice energy; part of the difficulty in making bond energy calculations for ionic solids is that the energy required to completely dissociate the solid into the gas phase corresponds to the atomization energy of the solid. This is not the same as the lattice energy of the solid, which refers to the energy of the crystal relative to *ions* in the gas phase. However, by having a correction factor, f, in equation (8.30) which is constant at $f = 1$ for halides and at $f = 0.63$ for oxides, Sanderson obtained good agreement between experimental and calculated bond energies using equation (8.30). Some examples are given in Table 8.13.

Table 8.13 *Bond energies*

Compound	n	$-\delta_x^*$	E_{calc} (kJ mol^{-1})	E_{exp} (kJ mol^{-1})
Li_2O	6	0.80	1172	1168
Na_2O	4	0.80	851	881
K_2O	4	0.84	777	791
Rb_2O	4	0.86	762	743
Cs_2O	4	0.90	721	723
BeO	4	0.42	1174	1175
MgO	4	0.50	1020	1040
CaO	4	0.57	1038	1061
SrO	4	0.60	1007	1002
BaO	4	0.67	958	982
LiF	3	0.74	869	852
NaF	3	0.75	766	760
KF	4	0.84	736	735
RbF	4	0.86	711	710
CsF	4	0.90	688	688
BeF_2	3	0.34	1462	1502
MgF_2	4	0.41	1499	1471
CaF_2	4	0.47	1546	1549
SrF_2	4	0.50	1522	1534
BaF_2	4	0.57	1532	1533

* Partial charge on anion.

8.3.6 Bond energies and structure

In order to illustrate how bond energy may influence the structure adopted by a particular compound some clear-cut examples are needed. Consider the long-standing question mark over the enormous difference in the structure of CO_2 and SiO_2. One is a gas, the other a high melting solid. And yet carbon and silicon are adjacent elements in Group IV of the periodic table and are expected to show many similarities in their physical and chemical properties. Clearly, CO_2 must be more stable as a molecule that contains two carbon–oxygen double bonds than as some other structure that contains four carbon–oxygen single bonds.

Although double bonds are stronger than single bonds they are not normally regarded as being at least twice as strong; however, clearly, they must be so in the case of CO_2. Why should this be? Sanderson's calculations indicate the answer to this and other questions, only a brief summary of which can be given here.

As mentioned in Section 8.3.5, the elements N, O and F exhibit the 'lone pair bond weakening effect' such that their single bond energies are considerably less than expected. The explanation that has previously been given is that the presence of lone pairs on adjacent atoms causes a kind of steric hindrance and hence repulsion between the atoms which leads to a weakening of the bond. Sanderson argues that this explanation must be incorrect—e.g. the N—H bonds in ammonia are also weakened but the hydrogen atom has no lone pairs—and that,

instead, the lone pairs must act towards screening off the effective nuclear charge of the atoms from the valence electrons. This leads to a reduction in bond energy by effectively reducing the electronegativity of the atoms (equation 8.28). Using correlations such as shown in Fig. 8.6, unweakened single bond energies were estimated. For oxygen this value, E''', 434 kJ mol^{-1}, is about three times the value of the oxygen–oxygen single bond energy determined experimentally from the dissociation of H_2O_2, 142 kJ mol^{-1}. Further, the dissociation energy of oxygen gas molecules, requiring cleavage of the double bond is 498 kJ mol^{-1}.

Recognition of the lone pair bond weakening effect in N, O and F leads to explanations of many phenomena:

(a) Oxygen is a diatomic gas whereas sulphur is a polymeric solid: one O=O double bond is stronger than two O—O single bonds. The lone pair bond weakening effect is much reduced in sulphur (and P, Cl, etc.), for which two single bonds are stronger than one double bond.
(b) Similarly, N_2 is a diatomic gas whereas P is a polymeric solid.
(c) The bond dissociation energy of fluorine is much less than that of chlorine: here there is no possibility of forming double bonds and direct comparison between the halogen single bond energies is possible. The reduced F—F bond energy accounts in large part for the high reactivity of fluorine.
(d) Carbon dioxide is a molecular gas whereas silica is a polymeric solid. Using data on the electronegativities and double bond energies of carbon and oxygen, the total dissociation energy of CO_2 was calculated by Sanderson, using the sequence of steps outlined above, to be 1608 kJ mol^{-1}. This is in close agreement with the experimental atomization energy of CO_2. On the other hand, for a hypothetical polymeric structure containing four C—O single bonds per carbon, the calculated dissociation energy is less, 1413 kJ mol^{-1}. Hence CO_2 prefers to exist as a triatomic molecule. (The dissociation energy of O_2 is 498 kJ mol^{-1}; this value is also regarded as being reduced, by the presence of one lone pair on each oxygen. The unweakened double bond energy is estimated as 574 kJ mol^{-1} and hence the value per oxygen atom, E'', is half, i.e. 287 kJ mol^{-1}.)

For SiO_2, the lone pair bond weakening effect is less important for two reasons: (i) the bond weakening effect influences only the covalent contribution and as silicon is more electropositive than carbon the Si—O bond is more ionic than the C—O bond; (ii) silicon has vacant *d* orbitals which allow partial double bonding to occur by donation of the lone pair of electrons on oxygen. Hence the single bond energy of oxygen is less weakened when bonded to silicon than when bonded to carbon. For calculations on SiO_2, Sanderson found it necessary to use the E'' value of 287 kJ mol^{-1} in order to obtain a dissociation energy for polymeric SiO_2 of 1859 kJ mol^{-1}, which was in good agreement with the experimental value. By contrast, calculations on the 'SiO_2 molecule' containing Si=O double bonds gave a much smaller dissociation energy, 1264 kJ mol^{-1}. Hence SiO_2 shows a clear preference for a polymeric structure with Si—O single bonds.

8.3.7 Some final comments on Sanderson's approach

Sanderson has extended his semi-empirical calculations on electronegativities and partial charges of atoms to the calculation of bond energies in polar materials (Section 8.3.6). This is a considerable advance on what has been possible using other methods. However, it has not been possible to make these calculations on a purely *ab initio* basis and the values of certain parameters have been chosen so as to give good agreement between experiment and calculation; one example is the *n* value used in covalent bond energy calculations on solids. Sanderson acknowledges that his calculations suffer from certain drawbacks and that, to a certain extent, some of his arguments are circular. However, these disadvantages appear to be more than outweighed by the increased understanding of bonding in solid materials which has resulted from these calculations and in particular by the quantization of concepts such as partial charge on atoms, bond ionicities and electronegativity equalization.

8.4 Mooser–Pearson plots and ionicities

While the radius ratio rules appear to be rather unsatisfactory for predicting and explaining the structure adopted by, for instance, particular AB compounds, an alternative approach by Mooser and Pearson (1959) has had considerable success. This approach focuses on the directionality or covalent character of bonds. The two factors which are regarded as influencing covalent bond character in crystals are (a) the average principle quantum number, $\bar{n}$, of the atoms involved and (b) their difference in electronegativity, Δx. In constructing

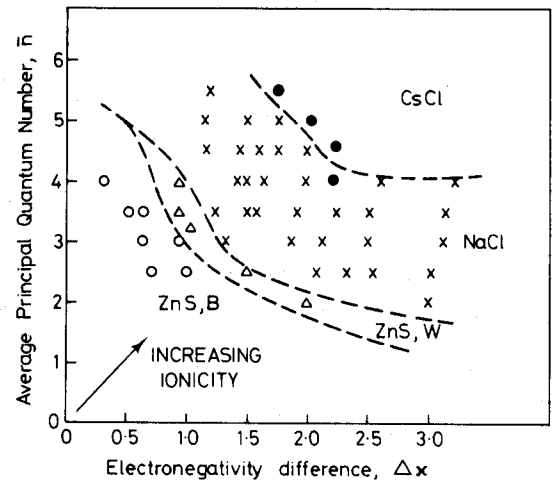

Fig. 8.7 Mooser–Pearson plot for AB compounds containing A group cations. (From Mooser and Pearson, 1959.) Arrow indicates direction of increasing bond ionicity

Mooser–Pearson plots, these two parameters are plotted against each other, as shown for AB compounds in Fig. 8.7. The most striking feature of the plot is the almost perfect separation of compounds into four groups corresponding to the structure: zinc blende (ZnS, B), wurtzite (ZnS, W), rock salt and CsCl. Similarly, successful diagrams have been presented for other formula types—AB_2, AB_3, etc. Of the four simple AB structure types, one's intuitive feeling is that zinc blende (or sphalerite) is the most covalent and either rock salt or CsCl is the most ionic. Mooser–Pearson plots present this intuitive feeling in diagrammatic form.

The term *ionicity* has been used to indicate the degree of ionic character in bonds; in Fig. 8.7, ionicity increases from the bottom left to the top right of the diagram, as shown by the arrow. Thus it appears that ionicity is not governed by electronegativity alone but also depends on the principal valence shell of the atoms and hence on atomic size. There is a general trend for highly directional covalent bonds to be associated with lighter elements, i.e. at the bottom of Fig. 8.7, and with small values of Δx, i.e. at the left-hand side of Fig. 8.7.

The fairly sharp crossover between the different 'structure fields' in Fig. 8.7 suggests that for each structure type there are critical ionicities which place a limit on the compounds that can have that particular structure. Theoretical support for Mooser–Pearson plots has come from the work of Phillips (1970) and van Vechten and Phillips (1970) who measured optical absorption spectra of some AB compounds and, from these, calculated electronegativities and ionicities. The spectral data gave values of band gaps, E_g (Chapter 14). For isoelectronic series of compounds, e.g. ZnSe, GaAs, Ge, the band gaps have contributions from (a) a homopolar band gap, E_h, as in pure germanium and (b) a charge transfer, C, between A and B, termed the 'ionic energy'. These are related by

$$E_g^2 = E_h^2 + C^2 \tag{8.31}$$

E_g and E_h are measured from the spectra and hence C can be calculated. C is related to the energy required for electron charge transfer in a polar bond and hence is a measure of electronegativity, as defined by Pauling. A scale of ionicity has been devised:

$$\text{Ionicity}, f_i = \frac{C^2}{E_g^2} \tag{8.32}$$

Values of f_i range from zero ($C = 0$ in a homopolar covalent bond) to one ($C = E_g$ in an ionic bond) and give a measure of the fractional ionic character of a bond. Phillips analysed the spectroscopic data for sixty-eight AB compounds with either octahedral or tetrahedral structures and found that the compounds fall into two groups separated by a critical ionicity, f_i, of 0.785.

The link between Mooser–Pearson plots and Phillips–Van Vechten ionicities is that

$$\Delta x\,(\text{Mooser–Pearson}) \simeq C\,(\text{Phillips})$$

and

$$\bar{n}\,(\text{Mooser–Pearson}) \simeq E_h\,(\text{Phillips})$$

The explanation of the latter is that as the principal quantum number of an element increases, the outer orbitals become larger and more diffuse and the energy differences between outer orbitals (s, p, d and /or f) decrease; the band gap, E_h, decreases until metallic behaviour occurs at $E_h = 0$. Use of $\bar{n}$ gives the average behaviour of anion and cation. The Phillips–Van Vechten analysis has so far been restricted to AB compounds but this has provided a theoretical justification for the more widespread use and application of the readily constructed Mooser–Pearson plots. Further developments in this area of crystal chemistry are anticipated; an enthusiastic and more detailed account is given by Adams (1974).

8.5 Bond valence and bond length

The structures of most *molecular* materials—organic and inorganic—may be satisfactorily described using valence bond theory in which single, double, triple and occasionally partial bonds occur between atoms. Difficulties rapidly arise, however, when valence bond theory is applied to crystalline, *non-molecular* inorganic materials, even though the bonding in them may be predominantly covalent. This is because there are usually insufficient bonding electrons available for each bond to be treated as an electron pair single bond. Instead, most bonds must be regarded as partial bonds.

An empirical but nevertheless useful approach to describing such bonds has been developed by Pauling, Brown, Shannon, Donnay and others and involves the evaluation of *bond orders* or *bond valences* in a structure. Bond valences are defined in a similar way to electrostatic bond strengths in Pauling's electrostatic valence rule for ionic structures (Section 8.2.2). As such, bond valences represent an extension of Pauling's rule to structures that are not necessarily ionic. Bond valences are defined empirically, using information on atom valences and experimental bond lengths; no reference is made, at least not initially, to the nature of the bonding, whether it be covalent or ionic or some blend of the two.

Pauling's electrostatic valence rule requires that the sum of the electrostatic bond strengths between an anion and its neighbouring cations should be equal in magnitude to the formal charge on the anion (equations 8.5 and 8.6). This rule may be modified to include structures which are not necessarily ionic by replacing (a) the electrostatic bond strength by the bond valence and (b) the formal charge on the anion by the valence of that atom (valence being defined as the number of electrons that take part in bonding). This leads to the *valence sum rule* which relates the valence, V_i, of atom i to the bond valence, b_{ij}, between atom i and neighbouring atom j; i.e.

$$V_i = \sum_j b_{ij} \tag{8.33}$$

Thus, the valence of an atom must be equal to the sum of the bond valences for all the bonds that it forms. For cases in which b_{ij} is an integer, this rule becomes the familiar rule that is used for evaluating the number of bonds around an atom in molecular structures, i.e. the valence of an atom is equal to the number of bonds

that if forms (counting double bonds as two bonds, etc.). In non-molecular, inorganic structures, however, integral bond valences are the exception rather than the rule.

The electrostatic bond strength in Pauling's rule is given simply by the ratio of cation charge: cation coordination number. Thus for structures in which the cation coordination is irregular or the cation–anion bonds are not all of the same length, only an average electrostatic bond strength is obtained. One advantage of the bond valence approach is that each bond is treated as an individual and hence irregularities or distortions in coordination environments can be taken into account.

For a given pair of elements, an inverse correlation between bond valence and bond length exists, as shown in Fig. 8.8 for bonds between oxygen and atoms of the second row in their group valence states, i.e. Na^{I}, Mg^{II}, Al^{III}, Si^{IV}, P^{V} and S^{VI}. While each atom and oxidation (or valence) state has its own bond valence–bond length curve, it is a considerable simplification that 'universal curves' such as Fig. 8.8 may be used for isoelectronic series of ions. Various analytical expressions have been used to fit curves such as Fig. 8.8, including

$$b_{ij} = \left(\frac{R_o}{R}\right)^N \tag{8.34}$$

where R is the bond length and R_o, N are constants (R_o is the value of the bond length for unit bond valence); for the elements represented by Fig. 8.8, $R_o = 1.622$ and $N = 4.290$.

From Fig. 8.8, bond length clearly increases with decreasing bond valence and since, for a given atom, bond valence inevitably decreases with increasing coordination number, a correlation also exists between increasing coordination

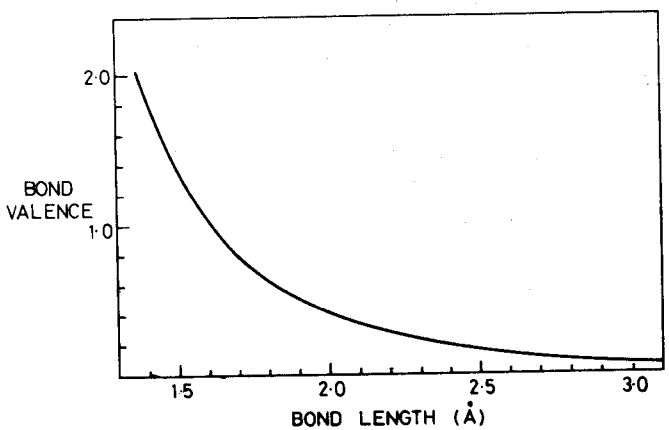

Fig. 8.8 Bond valence–bond length universal correlation curve for bonds between oxygen and second row atoms: Na, Mg, Al, Si, P and S. (From Brown, 1978)

number and increasing bond length. This correlation has already been presented, in a slightly different form, in Fig. 8.3, in which the ionic radii of cations increase with increasing coordination number. Since the data of Fig. 8.3 assume a constant radius of the fluoride or oxide ion, the ordinate in Fig. 8.3 could be changed from the ionic radius to the metal–oxygen bond length.

Curves such as Fig. 8.8 are important for several reasons, the most important of which is that they lead to an increased rationalization and understanding of crystal structures. They have several applications that are specifically associated with the determination of crystal structures; for example:

(a) As a check on the correctness of a proposed structure, the valence sum rule should be obeyed by all atoms of the structure to within a few per cent.
(b) To locate hydrogen atoms. Hydrogen atoms are often 'invisible' in X-ray structure determinations because of the very low scattering power of hydrogen. It may be possible to locate them by evaluating the bond valence sums around each atom and noting which atoms (e.g. oxygen atoms in hydrates) show a large discrepancy between the atom valence and the bond valence sum. The hydrogen is then likely to be bonded to such atoms.
(c) To distinguish between Al^{3+} and Si^{4+} positions in aluminosilicate structures. By X-ray diffraction, Al^{3+} and Si^{4+} cannot be distinguished because of their very similar scattering power, but in sites of similar coordination number they give different bond valences, e.g. in regular MO_4 tetrahedra, Si—O bonds have a bond valence of one but Al—O bonds have a bond valence of 0.75. Site occupancies may therefore be determined using the valence sum rule and/or by comparing the M—O bond lengths with values expected for Si—O and Al—O.

8.6 Non-bonding electron effects

In this section, the influence on structure of two types of non-bonding electrons is considered: the *d* electrons in transition metal compounds and the s^2 pair of electrons in compounds of the heavy *p*-block elements in low oxidation states. These two types of electrons do not take part in bonding as such, but nevertheless exert a considerable influence on the coordination number and environment of the metal atom.

8.6.1 *d* Electron effects

In transition metal compounds, the majority of the *d* electrons on the metal atom do not usually take part in bond formation but do influence the coordination environment of the metal atom and are responsible for properties such as magnetism. For present purposes, basic crystal field theory (CFT) is adequate to describe qualitatively the effects that occur. It is assumed that the reader is acquainted with CFT and only a summary will be given here.

8.6.1.1 *Crystal field splitting of energy levels*

In an octahedral environment, the five *d* orbitals on a transition metal atom are no longer degenerate but split into two groups, the t_{2g} group of lower energy and the e_g group of higher energy (Fig. 8.9a). If possible, electrons occupy orbitals singly, according to Hund's rule of maximum multiplicity. For d^4 to d^7 atoms or ions, two possible configurations occur, giving low spin (LS) and high spin (HS) states; these are shown for a d^7 ion in Fig. 8.10. In these, the increased energy, Δ, required to place an electron in an e_g orbital, and hence maximize the multiplicity, has to be balanced against the repulsive energy or pairing energy, *P*, which arises when two electrons occupy the same t_{2g} orbital. The magnitude of Δ depends on the ligand or anion to which the metal his bonded: for weak field anions, Δ is small and the HS configuration occurs, and vice versa for strong field ligands. Δ also depends on the metal and, in particular, to which row it belongs: generally

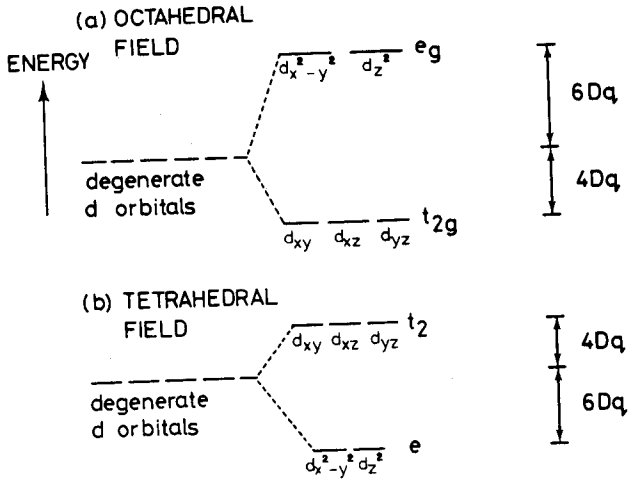

Fig. 8.9 Splitting of *d* energy levels in (a) an octahedral and (b) a tetrahedral field

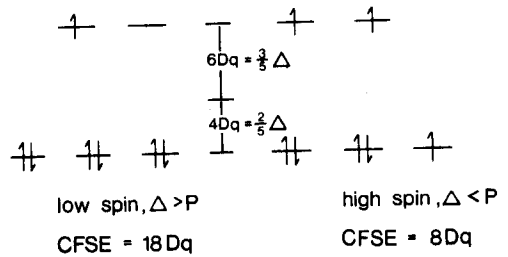

Fig. 8.10 Low spin and high spin states for a d^7 transition metal ion in an octahedral coordination environment

Table 8.14 *d Electron configuration in octahedrally coordinated metal atoms*

Number of electrons	Low spin, Δ > *P*. t_{2g}	e_g	High spin, Δ < *P* t_{2g}	e_g	Gain in orbital energy for low spin	Example
1	↑		↑			V^{4+}
2	↑ ↑		↑ ↑			Ti^{2+}, V^{3+}
3	↑ ↑ ↑		↑ ↑ ↑			V^{2+}, Cr^{3+}
4	↑↓ ↑ ↑		↑ ↑ ↑	↑	Δ	Cr^{2+}, Mn^{3+}
5	↑↓ ↑↓ ↑		↑ ↑ ↑	↑ ↑	2Δ	Mn^{2+}, Fe^{3+}
6	↑↓ ↑↓ ↑↓		↑↓ ↑ ↑	↑ ↑	2Δ	Fe^{2+}, Co^{3+}
7	↑↓ ↑↓ ↑↓	↑	↑↓ ↑↓ ↑	↑ ↑	Δ	Co^{2+}
8	↑↓ ↑↓ ↑↓	↑ ↑	↑↓ ↑↓ ↑↓	↑ ↑		Ni^{2+}
9	↑↓ ↑↓ ↑↓	↑↓ ↑	↑↓ ↑↓ ↑↓	↑↓ ↑		Cu^{2+}
10	↑↓ ↑↓ ↑↓	↑↓ ↑↓	↑↓ ↑↓ ↑↓	↑↓ ↑↓		Zn^{2+}

Δ(5*d*) > Δ(4*d*) > Δ(3*d*). Consequently HS behaviour is rarely observed in the 4*d* and 5*d* series. Δ values may be determined experimentally from electronic spectra. The possible spin configurations for the different numbers of *d* electrons are given in Table 8.14.

The radii of transition metal ions depend on their *d* electron configuration, as shown in Fig. 8.11(a) for the octahedrally coordinated divalent ions. With increasing atomic number, several trends occur. First, there is a gradual, overall decrease in radius as the *d* shell is filled, as shown by the dashed line that passes through Ca^{2+}, Mn^{2+}(HS) and Zn^{2+}. For these three ions, the distribution of *d* electron density around the M^{2+} ion is spherically symmetrical because the *d* orbitals are either empty (Ca), singly occupied (Mn) or doubly occupied (Zn). The gradual decrease in radius with increasing atomic number is associated with poor shielding of the nuclear charge by the *d* electrons; hence a greater effective nuclear charge is experienced by the outer, bonding electrons which results in a steady contraction in radius with increasing atomic number. Similar effects occur across any horizontal row of the periodic table as the valence shell is filled, but are particularly well documented for the transition metal series.

For the other ions d^1 to d^4 and d^6 to d^9, the *d* electron distribution is not spherical. The shielding of the nuclear charge by these electrons is reduced even further and the radii are smaller than expected. Thus, the Ti^{2+} ion has the configuration $(t_{2g})^2$, which means that two of the three t_{2g} orbitals are singly occupied. In octahedrally coordinated Ti^{2+}, these electrons (which are non-bonding) occupy regions of space that are directed away from the (Ti^{2+}–anion) axes. Comparing Ti^{2+} with Ca^{2+}, for instance, Ti^{2+} has an extra nuclear charge of +2 but the two extra electrons in the t_{2g} orbitals do not shield the bonding electrons from this extra charge. Hence, Ti—O bonds in, for example, TiO, are shorter than Ca—O bonds in CaO due to the stronger attraction between Ti^{2+} and the bonding electrons. This trend continues in V^{2+}, Cr^{2+}(LS), Mn^{2+}(LS) and Fe^{2+}(LS), all of which contain only t_{2g} electrons (Table 8.14). Beyond

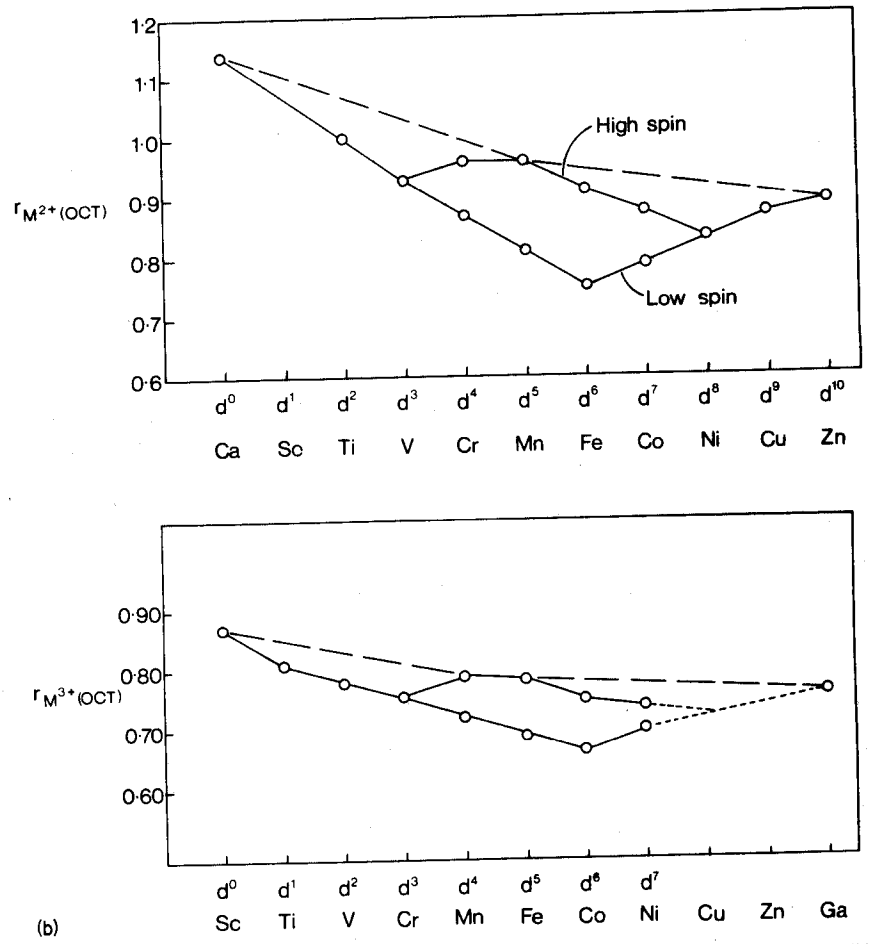

Fig. 8.11 (a) Radii of octahedrally coordinated divalent transition metal ions. (b) Radii of octahedrally coordinated trivalent transition metal ions. Data from Shannon and Prewitt, relative to $r_{F^-} = 1.19$ Å

Fe^{2+}(LS), the electrons begin to occupy e_g orbitals and these electrons do shield the nuclear charge much more effectively. The radii then begin to increase again in the series Fe^{2+}(LS), Co^{2+}(LS), Ni^{2+}, Cu^{2+} and Zn^{2+}

For the high spin ions a different trend is observed. On passing from V^{2+} to Cr^{2+}(HS) and Mn^{2+}(HS), electrons enter the e_g orbitals, thereby shielding the nuclear charge and giving rise to an increased radius. However, on passing from Mn^{2+}(HS) to Fe^{2+}(HS), Co^{2+}(HS) and Ni^{2+}, the additional electrons occupy t_{2g} orbitals and the radii decrease once again.

Trivalent transition metal ions show a similar trend but of reduced magnitude (Fig. 8.11b). However, the various effects that occur are now effectively transferred to higher atomic number and hence to the right by one atom; thus, the ion with the smallest radius is Co^{3+}(LS) instead of Fe^{2+}(LS).

So far, only octahedral coordination of transition metal ions has been considered. Tetrahedral coordination is also quite common but a different energy level diagram applies to the *d* electrons. A tetrahedral field also splits the *d* orbitals into two groups, but in the opposite manner to an octahedral field. Thus, three orbitals have higher energy d_{xy}, d_{xz} and d_{yz} whereas the other two, $d_{x^2-y^2}$ and d_{z^2} have lower energy (Fig. 8.9b).

It was mentioned in Section 8.2.7 that crystal field splitting of *d* orbitals in transition metal ions may result in *crystal field stabilization energies* (CFSE) and increased lattice energies of ionic compounds. For example, CoF_2 has the rutile structure with octahedrally coordinated $Co^{2+}(d^7)$ ions in which Co^{2+} adopts the high spin configuration (Fig. 8.10). The energy difference, Δ, between t_{2g} and e_g orbitals is set equal to 10 Dq and the t_{2g} orbitals are stabilized by an amount 4 Dq whereas the e_g orbitals are destabilized by an amount 6 Dq. Relative to the situation of five degenerate orbitals without crystal field splitting (Fig. 8.9), the crystal field stabilization energy of Co^{2+} in HS and LS states may be calculated. For the LS state, the CFSE is $6 \times 4\,Dq - 1 \times 6\,Dq = 18\,Dq$. For the HS state, the CFSE is $5 \times 4\,Dq - 2 \times 6\,Dq = 8\,Dq$.

The occurrence of CFSE leads to an increased lattice energy. The value of the CFSE calculated for Co^{2+}(HS) in rutile is 104 kJ mol^{-1}. This compares fairly well with the value of 83 kJ mol^{-1} given by the difference between the lattice energy determined from a Born–Haber cycle (2959 kJ mol^{-1}) and that calculated using the Born–Mayer equation (2876 kJ mol^{-1}).

The lattice energies of the divalent fluorides of the first row transition elements, determined from a Born–Haber cycle, are shown in Fig. 8.12. Similar trends are

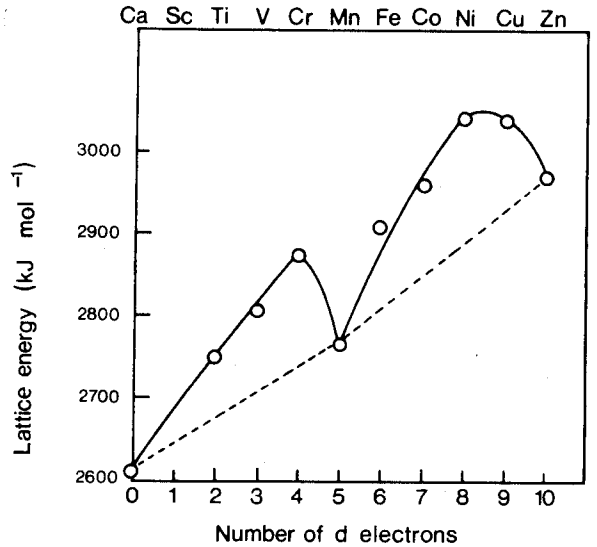

Fig. 8.12 Lattice energies of divalent transition metal fluorides determined from Born–Haber cycle calculations. (From Waddington, 1959)

observed for other halides. Ions that do not exhibit CFSE are d^0(Ca), d^5(HS)(Mn) and d^{10}(Zn), and their lattice energies fall on the lower, dashed curve. Most ions do show some degree of CFSE, however, and their lattice energies fall on the upper, solid curve. For the fluorides (Fig. 8.12), the agreement between the calculated CFSE and the difference in lattice energy ΔU [i.e. U(Born–Haber) – U(Born–Mayer)] is reasonable and indicates that the bonding may be treated as ionic. For the other halides, however, $\Delta U \gg$ CFSE and indicates that other effects, perhaps covalent bonding, must be present.

8.6.1.2 *Jahn–Teller distortions*

In many transition metal compounds, the metal coordination is distorted octahedral and the distortions are such that the two axial bonds are either shorter than or longer than the other four bonds. The Jahn–Teller effect is responsible for these distortions in d^9, d^7(LS) and d^4(HS) ions. Consider the d^9 ion Cu^{2+} whose configuration is $(t_{2g})^6(e_g)^3$. One of the e_g orbitals contains two electrons and the other contains one. The singly occupied orbital can be either d_{z^2} or $d_{x^2-y^2}$ and in a free ion situation both would have the same energy. However, since the metal coordination is octahedral the e_g levels, with one doubly and one singly occupied orbitals, are no longer degenerate. The e_g orbitals are high energy orbitals (relative to t_{2g}) since they point directly towards the surrounding ligands and the doubly occupied orbital will experience stronger repulsions and hence have somewhat higher energy than the singly occupied orbital. This has the effect of lengthening the metal–ligand bonds in the directions of the doubly occupied orbital, e.g. if the d_{z^2} orbital is doubly occupied, the two metal–ligand bonds along the z axis will be longer than the other four metal–ligand bonds. The energy level diagram for this latter situation is shown in Fig. 8.13(a). Lengthening of the metal–ligand bond along the z axis leads to a *lowering* of energy of the d_{z^2} orbital. The distorted structure is stabilized by an amount $\frac{1}{2}\delta_2$ relative to the regular octahedral arrangement and, hence, the distorted structure becomes the observed, ground state.

High spin d^4 and low spin d^7 ions also have odd numbers of e_g electrons and show Jahn–Teller distortions. It is not clear which type of distortion is preferred

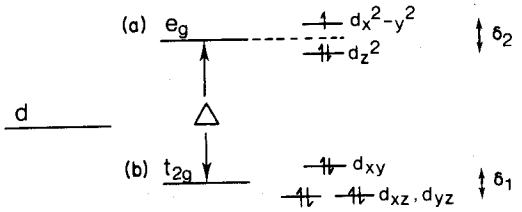

Fig. 8.13 Energy level diagram for the d-levels in a d^9 ion experiencing a Jahn–Teller distortion. The two bonds parallel to z are longer than the other four

(i.e. two short and four long bonds, or vice versa) and the actual shapes in a particular structure must be determined experimentally. The degeneracy of the t_{2g} levels may also be removed by the Jahn–Teller effect, but the magnitude of the splitting, δ_1 in Fig. 8.13(b), is small and the effect is relatively unimportant.

The normal coordination environment of the Cu^{2+} ion is distorted octahedral with four short and two long bonds. The distortion varies from compound to compound. In, for example, CuF_2 (distorted rutile structure), the distortion is fairly small (four fluorine atoms at 1.93 Å, two at 2.27 Å), but is larger in $CuCl_2$ (four chlorine atoms at 2.30 Å, two at 2.95 Å) and extreme in tenorite, CuO, which is effectively square planar (four oxygen atoms at 1.95 Å, two at 2.87 Å).

The importance of Jahn–Teller distortions in Cu^{2+} and Cr^{2+} (d^4 ion) compounds is seen by comparing the structures of the oxides and fluorides of the first-row divalent, transition metal ions. For the oxide series, MO(M^{2+} is Ti, V, Cr, Mn, Fe, Co, Ni and Cu), all have the rock salt structure with regular octahedral coordination apart from (a) CuO which contains grossly distorted (CuO_6) octahedra and possibly (b) CrO, whose structure is not known. For the fluoride series, MF_2, all have the regular rutile structure apart from CrF_2 and CuF_2 which have distorted rutile structures.

Other examples of distorted octahedral coordination due to the Jahn–Teller effect are found in compounds of Mn^{3+}(HS) and Ni^{3+}(LS).

8.6.1.3 *Square planar coordination*

The d^8 ions—Ni^{2+}, Pd^{2+}, Pt^{2+}—commonly have square planar or rectangular planar coordination in their compounds. In order to understand this, consider the d energy level diagram for such ions in (a) octahedral and (b) distorted octahedral fields:

(a) The normal configuration of a d^8 ion in an octahedral field is $(t_{2g})^6(e_g)^2$. The two e_g electrons singly occupy the d_{z^2} and $d_{x^2-y^2}$ orbitals, which are degenerate, and the resulting compounds, with unpaired electrons, are paramagnetic.

(b) Consider, now, the effect of distorting the octahedron and lengthening the two metal–ligand bonds along the z axis. The e_g orbitals lose their degeneracy, and the d_{z^2} orbital becomes stabilized by an amount $\frac{1}{2}\delta_2$ (Fig. 8.13). For small elongations along the z axis, the pairing energy required to doubly occupy the d_{z^2} orbital is larger than the energy difference between d_{z^2} and $d_{x^2-y^2}$, i.e. $P > \delta_2$. There is no gain in stability if the d_{z^2} orbital is doubly occupied, therefore, and no reason why small distortions from octahedral coordination should be stable. With increasing elongation along the z axis, however, a stage is reached where $P < \delta_2$ and in which the doubly occupied d_{z^2} orbital becomes stabilized and is the preferred ground state for a d^8 ion. The distortion from octahedral coordination is now sufficiently large that the coordination is regarded as square planar; in many cases, e.g. PdO, there are, in fact, no axial ligands along z and, hence, the transformation from

octahedral to square planar coordination is complete. Because they have no unpaired electrons, square planar compounds are diamagnetic.

Square planar coordination is more common with 4*d* and 5*d* transition elements than with 3*d* elements because the 4*d* and, especially, 5*d* orbitals are more diffuse and extend to greater radial distances from the nucleus. Consequently, the magnitude of the crystal (or ligand) field splitting (Δ, δ) caused by a particular ligand, e.g. O^{2-}, increases in the series $3d < 4d < 5d$. Thus, NiO has the rock salt structure with regular octahedral coordination of Ni^{2+}(3*d* ion) whereas PdO and PtO both have square planar coordination for the metal atoms (4*d* and 5*d*). The only known compound of palladium with octahedral Pd^{2+} is PdF_2 (rutile structure) and no octahedral Pt^{2+} or Au^{3+} compounds are known.

8.6.1.4 *Tetrahedral coordination*

As stated earlier, a tetrahedral field causes splitting of the *d* energy levels, but in the opposite sense to an octahedral field (Fig. 8.9b). Further, the magnitude of the splitting, Δ, is generally less in a tetrahedral field since none of the *d* orbitals point directly towards the four ligands. Rather, the d_{xy}, d_{xz} and d_{yz} orbitals are somewhat closer to the ligands than are the other two orbitals, Fig. 8.14 (only two orbital directions, d_{yz} and $d_{x^2-y^2}$ are shown). Jahn–Teller distortions again occur, especially when the upper t_2 orbitals contain 1, 2, 4 or 5 electrons (i.e. d^3(HS), d^4(HS), d^5 and d^9). Details will not be given since various types of distortion are possible (e.g. tetragonal or trigonal distortions) and these have not been as well studied as have the octahedral distortions. A common type of distortion is a flattening or elongation of the tetrahedron in the direction of one of the twofold axes of the tetrahedron (e.g. along *z* in Fig. 8.14). An example is the flattened $CuCl_4$ tetrahedron in Cs_2CuCl_4.

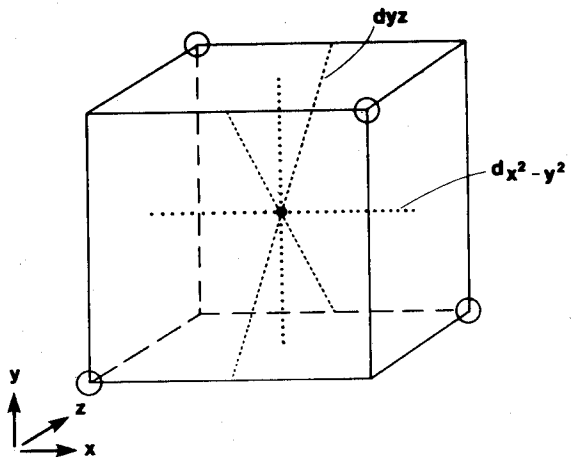

Fig. 8.14 The orientation of *d* orbitals in a tetrahedral field

8.6.1.5 *Tetrahedral versus octahedral coordination*

Most transition metal ions prefer octahedral coordination or a distorted variant of octahedral and an important factor is their large CFSE in octahedral sites. This can be estimated as follows. In octahedral coordination, each t_{2g} electron experiences a stabilization of $(4/10)\Delta^{oct}$ and each e_g electron a destabilization of $(6/10)\Delta^{oct}$. Thus Cr^{3+}, $d^3(t_{2g}^3)$ has a CFSE of $1.2\Delta^{oct}$ whereas Cu^{2+} $d^9(t_{2g})^6(e_g)^3$, has a CFSE of $0.6\Delta^{oct}$. In tetrahedral coordination, each *e* electron has a stabilization of $(6/10)\Delta^{tet}$ and each t_2 electron has a destabilization of $(4/10)\Delta^{tet}$ (Fig. 8.9). Thus, Cr^{3+} would have a CFSE of $0.8\Delta^{tet}$ and Cu^{2+} would have a CFSE of $0.4\Delta^{tet}$. With the guideline that

$$\Delta^{tet} \simeq 0.4\Delta^{oct}$$

the values of Δ^{oct} and Δ^{tet} for ions may be used to predict site preferences. More accurate values may be obtained spectroscopically and are given in Table 8.15 for some oxides of transition metal ions. It can be seen that high spin d^5 ions, as well as d^0 and d^{10} ions, have no particular preference for octahedral or tetrahedral sites insofar as crystal field effects are concerned. Ions such as Cr^{3+}, Ni^{2+} and Mn^{3+} show the strongest preference for octahedral coordination: thus tetrahedral coordination is rare for Ni^{2+}

The coordination preferences of ions are shown by the type of spinel structure that they adopt. Spinels have the formula AB_2O_4 and may be:

(a) normal—A tetrahedral, B octahedral;
(b) inverse—A octahedral, B tetrahedral and octahedral;
(c) some intermediate between normal and inverse.

The parameter, γ, is the fraction of A ions on octahedral sites. For normal spinels, $\gamma = 0$; for inverse, $\gamma = 1$; and for a random arrangement of A and B ions, $\gamma = 0.67$. Lattice energy calculations show that, in the absence of CFSE effects, spinels of the type 2, 3 (i.e. $A = M^{2+}$, $B = M^{3+}$, e.g. $MgAl_2O_4$) tend to be normal whereas

Table 8.15 *Crystal field stabilization energies (kJ mol^{-1}) estimated for transition metal oxides.* (Data from Dunitz and Orgel, 1960)

Ion		Octahedral stabilization	Tetrahedral stabilization	Excess octahedral stabilization
Ti^{3+}	d^1	87.4	58.5	28.9
V^{3+}	d^2	160.1	106.6	53.5
Cr^{3+}	d^3	224.5	66.9	157.6
Mn^{3+}	d^4	135.4	40.1	95.3
Fe^{3+}	d^5	0	0	0
Mn^{2+}	d^5	0	0	0
Fe^{2+}	d^6	49.7	33.0	16.7
Co^{2+}	d^7	92.8	61.9	30.9
Ni^{2+}	d^8	122.1	35.9	86.2
Cu^{2+}	d^9	90.3	26.8	63.5

Table 8.16 *The γ parameters of some spinels.* (Data from Greenwood, 1968 and Dunitz and Orgel, 1960)

M^{3+} \ M^{2+}	Mg^{2+}	Mn^{2+}	Fe^{2+}	Co^{2+}	Ni^{2+}	Cu^{2+}	Zn^{2+}
Al^{3+}	0	0.3	0	0	0.75	0.4	0
Cr^{3+}	0	0	0	0	0	0	0
Fe^{3+}	0.9	0.2	1	1	1	1	0
Mn^{3+}	0	0	0.67	0	1	0	0
Co^{3+}	—	—	—	0	—	—	0

spinels of type 4, 2 (i.e. $A = M^{4+}$, $B = M^{2+}$, e.g. $TiMg_2O_4$) tend to be inverse. However, these preferences may be changed by the intervention of CFSE effects, as shown by the γ parameters of some 2, 3 spinels in Table 8.16. Examples are:

(a) All chromate spinels contain octahedral Cr^{3+} and are normal. This is consistent with the very large CFSE of Cr^{3+} and ions such as Ni^{2+} are forced into tetrahedral sites in $NiCr_2O_4$.
(b) Most 2, 3 Mg^{2+} spinels are normal apart from $MgFe_2O_4$ which is essentially inverse. This reflects the lack of any CFSE for Fe^{3+}.
(c) $Co_3O_4 (\equiv CoO \cdot Co_2O_3)$ is normal because low spin Co^{3+} gains more CFSE by going into the octahedral site than Co^{2+} loses by occupying the tetrahedral site. Mn_3O_4 is also normal. Magnetite, Fe_3O_4, however, is inverse because whereas Fe^{3+} has no CFSE in either tetrahedral or octahedral coordination, Fe^{2+} has a preference for octahedral sites.

Spinels usually have cubic symmetry but some show tetragonal distortions in which one of the cell edges is of a different length to the other two. The Jahn–Teller effect gives rise to such distortions in Cu^{2+} containing spinels, $CuFe_2O_4$ (the tetragonal unit cell parameter ratio, $c/a = 1.06$) and $CuCr_2O_4 (c/a = 0.91)$. $CuFe_2O_4$ is an inverse spinel with octahedral Cu^{2+} ions and the Jahn–Teller effect distorts the CuO_6 octahedra so that the two Cu—O bonds along z are longer than the four Cu—O bonds in the xy plane. On the other hand, $CuCr_2O_4$ is normal and the CuO_4 tetrahedra are flattened in the z direction, again due to the Jahn–Teller effect, thereby causing a shortened c axis.

8.6.2 Inert pair effect

The heavy, post-transition elements, especially Tl, Sn, Pb, Sb and Bi exhibit, in some compounds, a valence that is two less than the group valence (e.g. the divalent state in Group IV elements, Sn and Pb). This is the so-called 'inert pair effect' and manifests itself structurally by a distortion of the metal ion coordination environment. Thus, Pb^{2+} has the configuration: (Xe core) $4f^{14}5d^{10}6s^2$, and the $6s^2$ pair is 'stereochemically active' in that these electrons are not in a spherically symmetrical orbital but stick out to one side of the Pb^{2+} ion (perhaps in some kind of s–p hybridized orbital).

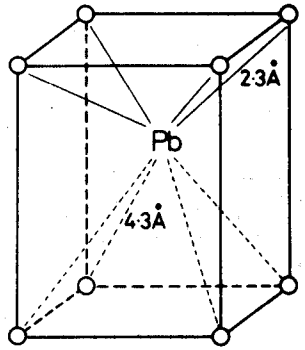

Fig. 8.15 The structure of red PbO showing the presence of the inert pair effect by the variation in Pb—O bond distances

Various kinds of distorted coordination polyhedra occur. Sometimes, the lone pair comes between the metal ion and some of its immediate anionic neighbours and causes a variation of bond length about the metal ion, e.g. red PbO has a structure that is a tetragonal distortion of the CsCl structure (Fig. 8.15). Four oxygens are situated at 2.3 Å from the Pb^{2+} ion, which is a reasonable Pb—O bond length, but the other four oxygens are at 4.3 Å. Although the lone pair is not directly visible, its presence is apparent from the distorted nature of the cubic coordination of Pb^{2+}.

A related distortion occurs in SnS which has a distorted rock salt structure. In this case, the SnS_6 octahedra are distorted along a [111] direction such that three sulphur atoms on one side of the tin are at ~ 2.64 Å but the other three are repelled by the lone pair to a distance of ~ 3.31 Å.

Another common kind of distortion occurs when the lone pair simply takes the plane of an anion and its associated pair of bonding electrons. Five-coordinated structures result in, for example, TlI, in which one corner (anion) of the octahedron 'TlI_6' is missing.

Questions

8.1 The oxides MnO, FeO, CoO, NiO all have the cubic rock salt structure with octahedral coordination of the cations. The structure of CuO is different and contains grossly distorted CuO_6 octahedra. Explain.
8.2 While the d electrons in many transition metal compounds may not be involved directly in bond formation, they nevertheless exert a considerable influence on structure. Explain.
8.3 The mineral grossular, $Ca_3Al_2Si_3O_{12}$ has the garnet structure, Chapter 16, with 8-coordinate Ca, octahedral Al and tetrahedral Si. Determine the probable coordination number and environment of oxygen and show that the structure obeys Pauling's electrostatic valency rule.

8.4 The most stable oxide of lithium is Li_2O but for rubidium and caesium, the peroxides M_2O_2 and superoxides MO_2 are more stable than the simple oxides M_2O. Explain.

8.5 BeF_2 has the same structure as SiO_2, MgF_2 is the same as rutile and CaF_2 has the fluorite structure. Does this seem reasonable?

8.6 Account for the observation that whereas CuF_2 and CuI are stable compounds, CuF and CuI_2 are not stable.

8.7 In Table 7.5 are given unit cell constants for some oxides MO with the rocksalt structure. Assuming that (i) $r_{O^{2-}} = 1.26$ Å; (ii) $r_{O^{2-}} = 1.40$ Å, calculate for each (a) two values of the cation radius, $r_{M^{2+}}$, (b) two values for the radius ratio, $r_{M^{2+}}/r_{O^{2-}}$. Assess the usefulness of the radius ratio rules in predicting octahedral coordination for M^{2+} for these oxides. Repeat the calculations for two oxides with the wurtzite structure, Table 7.9.

8.8 Calculate lattice energy values for the alkaline earth oxides using Kapustinskii's equation and the data given in Table 7.5. Compare your results with those given in Table 8.6. Estimate the enthalpies of formation of these oxides.

8.9 Using Sanderson's methods, estimate the partial ionic character of the sodium halides. Hence calculate the radii of the atoms involved and the unit cell *a* value (all have the rock salt structure). Compare your answers with the data given in Table 7.5.

References

D. M. Adams (1974). *Inorganic Solids*, Wiley.

L. H. Ahrens (1952). The use of ionisation potentials. I, Ionic radii of the elements, *Geochim. Cosmochim. Acta*, **2**, 155–169.

I. D. Brown (1978). Bond valences—a simple structural model for inorganic chemistry, *Chem. Soc. Revs.*, **7** (3), 359.

I. D. Brown and R. D. Shannon (1973). Empirical bond strength–bond length curves for oxides, *Acta Cryst.*, **A29**, 266.

G. O. Brunner (1971). An unconventional view of the 'closest sphere packings', *Acta Cryst.*, **A27**, 388.

J. D. Dunitz and L. E. Orgel (1960). Stereochemistry of ionic solids, *Adv. Inorg. Radiochem.*, **2**, 1–60.

F. G. Fumi and M. P. Tosi (1964). Ionic sizes and Born repulsive parameters in the NaCl type alkali halides, *J. Phys. Chem. Solids*, **25**, 31–43.

N. N. Greenwood (1968). *Ionic Crystals, Lattice Defects and Nonstoichiometry*, Butterworths.

A. F. Kapustinskii, Lattice energy of ionic crystals, *Quart. Rev.*, **10**, 283–294.

H. Krebs (1968). *Fundamentals of Inorganic Crystal Chemistry*, McGraw-Hill.

J. Krug, H. Witte and E. Wölfel (1955). *Zeit. Phys. Chem., Frankfurt*, **4**, 36.

M. F. C. Ladd and W. H. Lee (1963, 1965). Lattice energies and related topics, *Progr. Solid State Chem.*, **1**, 37–82; **2**, 378–413.

G. J. Moody and J. D. R. Thomas, Lattice energy and chemical prediction. Use of the Kapustinskii equations and the Born–Haber cycle, *J. Chem. Educ.*, **42** (4), 204.

E. Mooser and W. B. Pearson (1959). On the crystal chemistry of normal valence compounds, *Acta Cryst.*, **12**, 1015–1022.

L. Pauling (1928). The sizes of ions and their influence on the properties of salt-like compounds, *Z. Krist.*, **67**, 377–404.

J. C. Phillips (1970). Ionicity of the chemical bond in crystals, *Rev. Modern Phys.*, **42**, 317–356.

R. T. Sanderson (1967). The nature of 'ionic' solids, *J. Chem. Ed.*, **44** (9), 516.

R. T. Sanderson (1976). *Chemical Bonds and Bond Energy*, Academic Press.

R. D. Shannon and C. T. Prewitt (1969, 1970). Effective ionic radii in oxides and fluorides, *Acta Cryst.*, **B25**, 725–945; **B26**, 1046.

Shih-Ming Ho and Bodie E. Douglas (1969). A system of notation and classification for typical close packed structures, *J. Chem. Ed.*, **46**, 207–216.

K. H. Stern and E. S. Amis (1959). Ionic size, *Chem. Revs.*, **59**, 1.

J. A. van Vechten and J. C. Phillips (1970). New set of tetrahedral covalent radii, *Phys. Rev.*, **B2**, 2160–2167.

T. C. Waddington (1959). Lattice energies and their significance in inorganic chemistry, *Adv. Inorg. Chem. Radiochem.*, **1**, 157–221.

T. C. Waddington (1966). Ionic radii and the method of the undetermined parameter, **62**, 1482–1492.

A. F. Wells (1975). *Structural Inorganic Chemistry*, 4th ed., Oxford.